Engineering Library

JOURNAL OF THE Electrochemical Society

LIBRARY
UNIVERSITY OF UTAH
JAN 12 1951
SALT LAKE CITY

Vol. 98, No. 1 January, 1951

Published Monthly by

THE ELECTROCHEMICAL SOCIETY

Journal of the

Electrochemical Society

JANUARY, 1951 VOLUME 98 • NUMBER 1

CONTENTS

Potentiometric Titrations Involving Solutions of Metals in Liquid Ammonia. *George W. Watt and John B. Otto, Jr.* 1
The Structure of Metal Deposits Obtained by Electrochemical Displacement upon Zinc. *M. E. Straumanis and C. C. Fang* 9
The Effect of Acoustical Radiations on the Hydrogen Electrode. *Ernest Yeager and Frank Hovorka* 14
The Formation of Molybdenum Disilicide Coatings on Molybdenum. *E. A. Beidler, C. F. Powell, I. E. Campbell, and L. F. Yntema* 21
Distribution of Current in Porous Electrodes. *J. J. Coleman* 26
Rate of Dissolution of Silver in Aqueous Ceric Sulfate Solutions. *Hugh W. Salzberg, Helen Knoetgen, and Ann M. Molless* 31

Technical Reviews

Some Historical Developments Relating to Corrosion. *Wilson Lynes* 3C

Feature Section

Volta and the Volt. *George W. Vinal* 11C

Current Affairs

Marine Corrosion Laboratory Dedicated 14C
Washington Plans Ninety-ninth Meeting 14C
Division News 15C
Section News 15C
Personals 17C
New Members 18C
Book Reviews 18C
Recent Patents 19C
Future Meetings of Other Organizations 20C
Notes from Industry 20C
Employment Situations 20C

H. H. Uhlig, *Editor*

Norman Hackerman, *Technical Editor* F. L. LaQue, *Business Manager* R. M. Burns, *Consultant*

Eleanor Reid, *Managing Editor* H. B. Linford, *Associate Editor* U. B. Thomas, *Associate Editor* R. G. Ellis, *Advertising Manager*

Divisional Editors

J. M. Bialosky, *Corrosion* Abner Brenner, *Electrodeposition* N. C. Cahoon, *Battery* H. C. Froelich, *Electronics*

W. C. Gardiner, *Industrial Electrolytic* A. E. Pavlish, *Electrothermic* R. R. Ralston, *Electric Insulation* W. D. Robertson, *Theoretical* Sherlock Swann, Jr., *Electro-Organic*

Published monthly by The Electrochemical Society, Inc., Mt. Royal and Guilford Aves., Baltimore 2, Md., combining the Journal and Transactions of The Electrochemical Society. Editorial Office: 235 W. 102nd St., New York 25, N. Y. Statements and opinions given in articles and papers in the Journal of The Electrochemical Society are those of the contributors, and The Electrochemical Society assumes no responsibility for them. Subscription: $8.50 to members, $12.00 to nonmembers. Single copies $1.00 to members, $1.25 to nonmembers. Copyright 1951 by The Electrochemical Society. Entered as second-class matter November 15, 1947, at the Post Office at Baltimore, Md., under the act of August 24, 1912.

Editorial

Season's Greetings

AS THE YEAR ENDS, reminiscences and recapitulation give way to plans for the New Year. A few things stand out on the national scene. The Korean war has cast a long shadow over a world already fatigued by continuing shocks and struggles, described by some as the birth-pains of emerging internationalism. The New Year provides no certain promise of change in this respect. However, whatever the world's problems, our plans must continue to recognize that solutions to these problems exist, and that it remains our obligation to find the answers and to contribute whatever effort is necessary in making the answers effective.

On the brighter side, the National Science Foundation has actively gotten under way. Production figures over all the nation reached a new high, in which electrochemistry played a major role. Education on a higher level has reached more people. And not least, the public conscience can still be aroused in defense of truth and good taste, as the television producers learned in launching their recent publicity.

Our Society has also made progress. The rate of increase in membership has gone up 35% over 1949; total membership shows a gain of 6%. With this issue of the new JOURNAL, marking the third birthday, figures show that we are receiving 20% more technical papers than a year ago, and the papers are better. Attendance at national conventions has increased, programs have been interesting, and the technical sessions more stimulating and better organized. Your officers have worked hard to build upon an improved foundation.

Many years ago, a wise man counseled as follows: "When you choose a wife, character is the first and indispensable quality. Then a good mind in a sound body, congenial tastes, education, and social capacity. Wealth, if possible, but at any rate an understanding of the importance of practical matters." Choosing a technical society is not in quite the same category as choosing a wife, but if editorial license permits, one can say at least that The Electrochemical Society has acquired all the "indispensable qualities" and continues a good choice. We cannot confess to wealth; in fact the very opposite is true, but a sense of the practical has governed every action from the increase in dues to modification of the Constitution.

The Society's outlook promises a Happy New Year—the same to all of you.

293477

Enthone chemists scientifically select the *Best Stripper* for each *individual* job

During the past 15 years Enthone has developed over a score of strippers for organic finishes, including nitrocellulose lacquers, alkyd, ureaformaldehyde and melamine synthetic enamels. Some strippers are used straight at room temperatures, require no rinsing and have no odor. Other strippers are used mixed with water. Strippers are available that do not attack any kind of base metal. All provide fast action and economy of operation.

If a standard stripper will not remove the coating on your work, a new one tailor-made to do the job will be formulated. To save time, fill out our questionnaire and return with samples for free laboratory service.

ENTHONE
INCORPORATED
442 Elm Street
New Haven, Conn.

NEW STRIPPER CIRCULAR MAILED ON REQUEST

Potentiometric Titrations Involving Solutions of Metals in Liquid Ammonia[1]

GEORGE W. WATT AND JOHN B. OTTO, JR.[2, 3]

Department of Chemistry, The University of Texas, Austin, Texas

ABSTRACT

A relatively simple apparatus for use in potentiometric titrations in which the titrating reagents consist of solutions of alkali metals (or alkaline earth metals) in liquid ammonia at −38°C is described, together with complete procedural and operational details. The utility of these methods has been demonstrated in the study of the formation of polyanionic salts by reactions between polysulfides of sodium, potassium, rubidium, and cesium in liquid ammonia and liquid ammonia solutions of the corresponding metals.

INTRODUCTION

Nearly twenty years ago, Zintl and co-workers (1) described a method for carrying out potentiometric titrations involving solutions of metals in liquid ammonia. These workers also reported results obtained by titrating ammonia solutions of compounds of elements in Groups I to VI in the periodic table with ammonia solutions of sodium. Of particular interest in connection with the present investigation is the fact that they reported evidence for the formation of salts of homopolyatomic anions (e.g., Na_2S_x, where x = 1-6 inclusive) by the non-transitional elements of Groups IV to VI inclusive. Probably owing to the complexity of the equipment described by Zintl, *et al.*, together with experimental difficulties inherent in the method, there appears to have been no subsequent application of this potentially very useful technique.

The present investigation was undertaken with a view to developing simplified equipment and procedures for such titrations. It was hoped thereby to make available a method which should be useful in the detection of intermediate oxidation states of the elements, in the study of the mechanism of the reduction of both inorganic and organic substances in liquid ammonia (2), in the study of acid-base reactions in ammonia, and numerous other applications. A secondary objective was to clear up uncertainties in the work of Zintl, *et al.*, particularly with reference to the existence of certain of the sodium polysulfides.

EXPERIMENTAL

All chemicals employed in this work were strictly anhydrous reagent grade materials which were analyzed by standard methods. All transfers were made in an anhydrous oxygen-free atmosphere.

Titration Equipment

The apparatus is shown diagrammatically and approximately to scale in Fig. 1. Several scales were used in this drawing because of space limitations. The cross-sectional view of the titrator[4] is approximately $\frac{1}{4}$ actual size; all tubing in the remainder of the drawing is about $\frac{1}{8}$ size. The vertical dimensions of the unfolded view of the titrator are approximately $\frac{1}{8}$ scale, and for all other parts, about $\frac{1}{14}$ scale. Capillary tubes K1, K2, and K3 are 2-mm bore.

The titrator is shown in Fig. 1 in both a semi-schematic unfolded view, and in a separate cross-sectional view in which the components are shown in the manner in which they are arranged with respect to the Dewar flask D, which is the housing for the essential parts of the titrator[4]. This flask (indicated by a dashed line in the unfolded view of the titrator) has the inside dimensions of about 7 x 30 cm and is used to contain refrigerant liquid ammonia and serves as the cooling bath for the titrator. The flask is provided with a liquid ammonia inlet, a fritted glass gas dispersion tube for stirring the refrigerant with a stream of predried air, a low temperature thermometer, and a gas outlet.

V is a calibrated container used to make up solutions of metals in liquid ammonia to known concentrations. This vessel is provided with a ground glass joint J1, through which the alkali metal sample is introduced after removal of cap C2, and a fritted glass gas dispersion cylinder F1, which serves to disperse the gas used to stir the solution and to filter the solution when it is transferred into buret B via T1 and K1. B is the titration buret from which metal solutions are added to the titration vessel R via T2 and K2. Vessel R, which contains a liquid ammonia solution of the substance being titrated, may be opened at J2 for the introduction of samples, and is provided with a fritted glass filter disc F2 which serves to disperse the gas used to

[1] Manuscript received July 11, 1950.

[2] Humble Oil and Refining Company Fellow, 1948–1949.

[3] Present address: Mound Laboratory, Monsanto Chemical Company, Miamisburg, Ohio.

[4] I.e., the volumetric vessel V, buret B, and reaction vessel R.

stir the solution. Electrodes E_i and E_r are connected to the minus and plus terminals, respectively, of a Leeds & Northrup No. 7651 potentiometer; the voltage measurement circuit is wired in the conventional manner and includes a calibrated (U.S.N.B.S.) standard cell.

Attached to the titrator are burets P1 and P2 which are essentially pressure regulating devices by means of which metal solutions are transferred from V to B, and thence into R.

Ammonia and nitrogen gas introduced into the system (at pressures indicated by manometer M) pass through fritted glass discs F3 and F4, respectively, and are scrubbed through Q (which contains a liquid ammonia solution of potassium) in order to remove the last traces of oxygen. Scrubber Q consists of a straight tube bearing a side arm addition bulb G for the introduction of solid potassium, and a gas dispersion cylinder F5; Q is cooled by means of liquid ammonia contained in a small Dewar flask which is provided with liquid ammonia inlet and gas outlet tubes.

All gases leave the system via manifold H from which they are discharged, after passing through bubbler L, either directly into the atmosphere or after scrubbing through absorbers containing acid to remove ammonia. The rate of discharge of gas is controlled in relation to the rate of bubbling through L, which contains mineral oil, and which serves not only to seal the exit gas system against back diffusion of air but also to equalize outlet pressures. A by-pass to S6 provides for evacuation without drawing the mineral oil back into the other parts of the system; trap N is simply an added safeguard.

Joint J3 provides for attachment of a small glass still used for purification of alkali metals by distillation *in vacuo* and the filling of small glass ampoules (1) with the metal samples that are subsequently introduced into V. J3 serves also as a point of attachment for a device (Fig. 2) used for filling the reference electrode compartment with anhydrous ammonia gas.

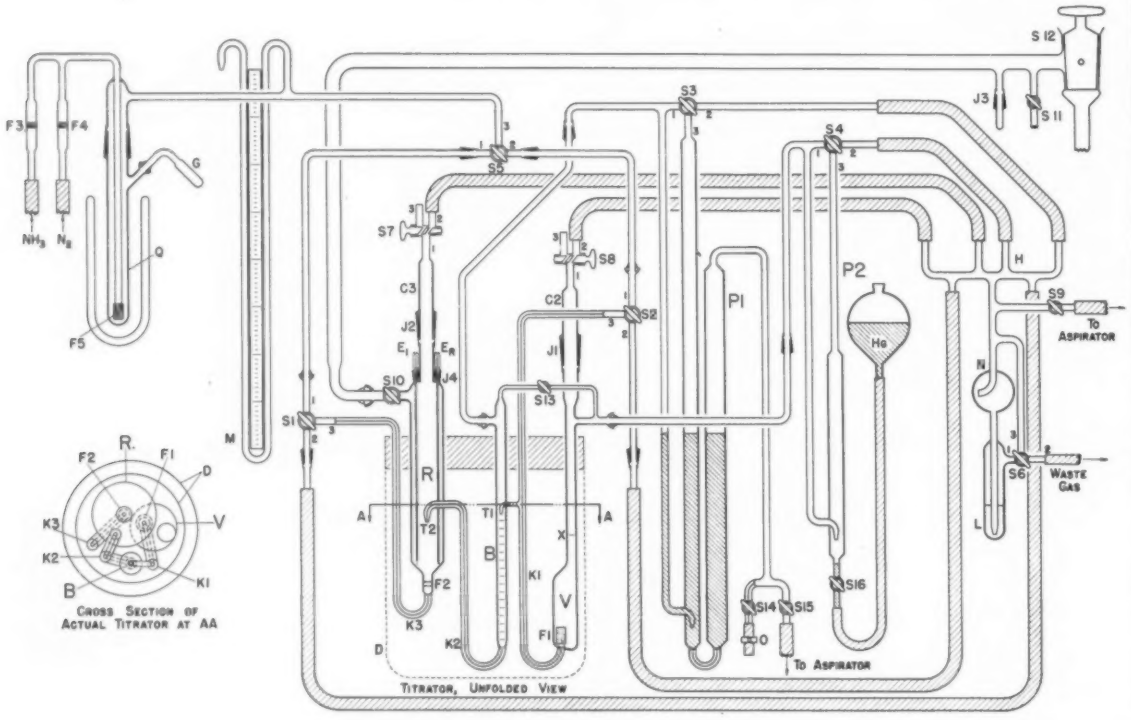

Fig. 1. Titrator and accessories

Certain other auxiliary equipment is not shown in Fig. 1. This includes a vacuum system which provides a means of evacuating the titrator and gas burets P1 and P2, the gas inlet and/or outlet system, and any other equipment attached at J3. Attachment of the main body of the apparatus to the vacuum system is via S11 (to a McLeod gauge) and via S12 to an oil pump supplemented by a mercury vapor diffusion pump. Liquid ammonia used as a refrigerant in the Dewar flasks surrounding Q and R, B, and V is drawn from a commercial cylinder,

collected for temporary storage in an intermediate Dewar flask, and dispensed in the manner described by Johnson and Fernelius (3).

The electrode system finally selected for use in the present work[5] consists of a clean platinum wire (E_i) which is immersed in the solution being titrated and a differential electrode (E_r) consisting of a modification of the type of electrode originally described by Muller (4) and shown in detail in Fig. 2*a*. For each titration the reference electrode compartment C is filled with a portion of the solution to be titrated; this is done in the manner described below.

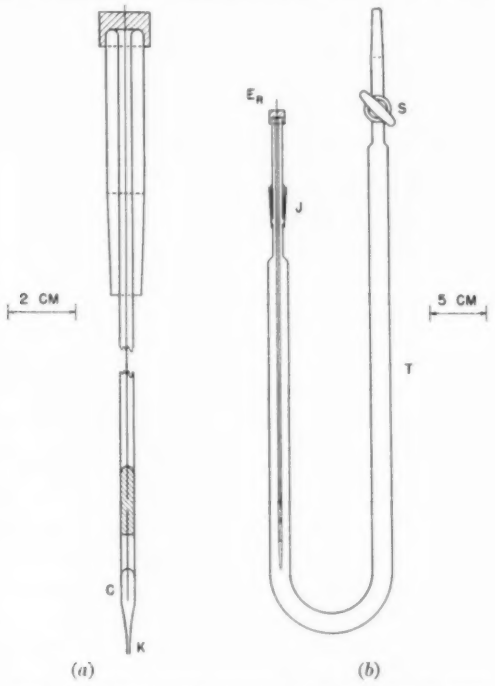

FIG. 2. (*a*) Reference electrode, E_r. (*b*) Device used for filling reference electrode with gaseous ammonia.

Preparation of Apparatus for Titration

Prior to the introduction of the reference electrode E_r into reaction vessel R of Fig. 1, the electrode compartment is filled with anhydrous ammonia gas as follows: E_r is inserted into tube T at ground joint J as shown in Fig. 2*b*, and the assembled apparatus shown in Fig. 2*b* is attached at J3 of Fig. 1, evacuated to about 10^{-5} mm, baked with a heat lamp to assist in degassing, and finally filled with anhydrous ammonia gas at a pressure of 1 atm via stopcock S. The electrode is maintained in this condition until needed for use in a titration, whereupon it is inserted into R (Fig. 1) in the manner described under *Procedure*. Except for the ammonia gas retained in the apparatus beyond stopcock S in Fig. 2*b*, that introduced into the system for the purpose of filling the electrode compartment is removed by means of a water aspirator via S9 of Fig. 1.

Approximately 2 g of potassium cut into small pieces is introduced into G, after which G is attached to Q.

With stopcocks S1, S2, S3, S4, and S5 in position 1,2,3; S6 in position 1,3; S7 and S8 in position 1,2; S10, S11, S12, S13, and S14 in the open position; and S9, S15, and S16 in the closed position, the entire system is evacuated (with the oil pump only) to a pressure of about 0.05 mm. Next, with stopcocks S1, S2, S3, and S4 changed to position 1,3, and S7 and S8 to the off position, the titrator, gas burets P1 and P2, and the gas inlet side of the system are evacuated to about 0.01 mm. Stopcock S5 is then changed to the 1,2 position and nitrogen is admitted to the gas inlet system to a pressure of 1 atm. Meanwhile, evacuation of the titrator and gas burets is continued by means of both the oil pump and the mercury vapor pump. At the same time, the titrator is baked with a heat lamp to facilitate drying. Stopcocks S11 and S12 are closed and nitrogen is admitted through S5 to all parts of the system except the gas exit system. Thereupon, S10 is closed and nitrogen is admitted to the gas exit system by putting S8 in position 1,2. This reduces the pressure in the titrator to less than atmospheric, but the pressure therein is brought back to atmospheric by adding more nitrogen through S5; S8 is then turned to the off position.

In this manner, the apparatus is prepared for introduction of samples into V and R. Stopcock S5 is placed in position 3,2; stopcock S8 is turned to position 1,2; and S6 is changed to position 1,2. While nitrogen is bubbled fairly rapidly through L, cap C2 is removed, S8 is turned to the off position, and in the shortest possible time the glass ampoule containing the alkali metal is lowered to the bottom of V by means of a wire slipped through a glass hook on the ampoule. The wire is quickly withdrawn and a crushing rod long enough to extend above J1 is inserted into V. S8 is changed to position 1,3 and C2 is reattached at J1. C2 is then swept out with nitrogen for at least 5 min, after which S8 is turned to the off position and the flow of nitrogen is cut off. S5 is turned to position 1,2 and the titrator and burets P1 and P2 are evacuated with the oil pump to about 0.005 mm, after which nitrogen is

[5] The use of bimetallic electrode systems (e.g., Pt vs. 90% Pt-10% Rh, and Pt vs. W) in preliminary experiments involving the titration of solutions of ammonium salts or alkali polysulfides with solutions of alkali metals gave results that were unreliable, as judged in terms of known end-points that could be detected visually with an error of the order of ±0.5 per cent.

again let into the system through S5 to a pressure of 1 atm.

By an identical sequence of operations, cap C3 is removed and the substances needed to make up the solution to be titrated in R are introduced. In the present studies these consist of a known weight of sulfur and a known weight of the appropriate alkali metal iodide contained in a fragile glass ampoule. The alkali iodides, which are readily soluble in ammonia, are added to increase the conductivity of the solution in R.

By the same procedure used in introducing the alkali metal into V, C2 is removed at J1, the bulb containing the alkali metal is quickly crushed, C2 is replaced, and the system is again evacuated and subsequently filled with nitrogen as before. By a similar procedure the bulb in R is crushed, but the system is not thereafter evacuated because this operation tends to carry finely divided solids up into S10, C3, and S7. With S5 in position 1,3 and S1 in position 1,2, refrigerant ammonia is transferred to the Dewar flask surrounding Q. While this is being done, nitrogen is put through the remainder of the system at a rate such as to prevent drawing a vacuum when Q is cooled by the refrigerant. Some or all of the potassium is transferred from G to Q and ammonia is condensed in Q until it is approximately ⅔ full of potassium solution. The flow of ammonia is turned off, S1 is changed to position 1,3; S7 to position 1,2, and nitrogen is put through while refrigerant ammonia is being brought into D. The refrigerant in D is stirred with dry air at a rate such that the temperature is lowered to about −36° C, and the nitrogen is replaced by ammonia which is condensed in R against the pressure head in L. After about 45 ml of ammonia are condensed, the ammonia is shut off, and nitrogen is bubbled through the solution in R until the space above the solution is filled with nitrogen saturated with ammonia; the flow of nitrogen is then stopped.

To condense ammonia in V, S5 is changed to position 3,2; S8 to position 1,2; and S7 and S13 are closed so that the path of gas flow is through V via F1. Ammonia is condensed in V to a point about 2 cm below the calibration mark X. Ammonia in the gas inlet stream is replaced by nitrogen which carries with it (from Q) enough residual ammonia to bring the volume up to X. This is an extremely delicate operation which requires adjustment of the temperature of D to the working temperature of −38° C, while at the same time manipulating the temperature of Q and the rate of gas flow so that the final solution in V fills it to, and only to, the calibration mark X when the gas stream is shut off and the metal solution rises in K1. In approaching completion of the condensation, trial readings are taken by opening S13; this allows solution to flow back into K1, with a meniscus at X. The total volume in V can be determined if the level of solution in K1 is within the range of the calibration marks on B, in terms of which K1 is calibrated[6].

The only additional operations necessary in preparation for the titration consist of filling gas burets P1 and P2 with nitrogen saturated with ammonia. This is done by changing S4 to position 3,2, closing S8, and opening S13 which allows the ammonia-free nitrogen in P2 to be replaced by nitrogen which becomes saturated with ammonia in its passage through Q. S3 is changed to position 1,2 and S4 is returned to position 1,3. A vacuum is pulled on P1 via S15 (with S14 closed) by means of a water aspirator in order to lower the level of the mercury in P1 below the level of the tip which enters P1 near the bottom by way of a ring seal. Then S15 is closed and the aspirator turned off. S3 is then turned to position 3,2, whereupon the ammonia-free nitrogen in P1 is replaced by nitrogen saturated with ammonia. S3 is returned to position 1,2; air is admitted through S14 until the level of the mercury in the right hand member of P1 is approximately 15 cm above the level in the left hand member[7]. Upon completion of these operations, S8 is turned to position 1,2; S3 is returned to position 1,3; and the flow of nitrogen is stopped; S5 is then moved to position 3,1 and S7 is placed in position 1,2. This permits the solution in R to be stirred by the nitrogen admitted via S1. At this stage the stopcock arrangement is as follows: S1, S2, S3, S4, and S5 in position 1,3; S6, S7, and S8 in position 1,2; S13 in the open position; and S9, S10, S11, S12, S14, S15, and S16 in the closed position, and the system is in condition for the actual titration.

Titration Procedure

The procedure given below is for the titration of a liquid ammonia solution of an alkali metal polysulfide, M_2S_x, with an ammonia solution of the corresponding alkali metal, M. This necessarily requires the *in situ* preparation of the polysulfide.

About one third of the metal solution in V is transferred to B for accurate measurement by placing S3 in position 1,2 (which allows gas in B to escape when it is displaced by solution), closing S8 and S13 and opening S16 slowly so as to admit mercury from the leveling bulb into P2 which compresses the gas therein and hence above the metal

[6] F1 does not fill with metal solution; hence, the true volume of solution in V is obtained by subtracting the volume of F1 from the volume of V read from a calibration curve in which the volume in V is plotted as ordinate against the buret reading express in milliliters.

[7] This condition is necessary to obviate too rapid transfer of metal solution from B to R.

solution in V. Metal solution flows from V through T1 via K1 into B. Flow is stopped by closing S16 and the pressure between B and V is equalized by opening S8 first, and then S13 which allows the solution in K1 to drop to a level equal to that in V; S3 is then returned to position 1,3.

The alkali polysulfide is next prepared by transferring from B to R a quantity of metal solution sufficient to give a composition M_2S_x where $x > 6$. This is done by closing S8 and S13 and cautiously opening S14 which allows air to enter the right hand member of P1 through O[8] and compresses the gas in the left member of P1 and hence above the solution in B and causes it to flow up K2 to T2, where the flow is stopped abruptly by closing S14. (If any drops fall from T2, which is drop-calibrated, they are counted, recorded, and subsequently added to the volume of metal solution added to R.) The reading of buret B is then taken with the solution in K2 just at the opening of tip T2. S14 is again cautiously opened and the desired quantity of metal solution is delivered into R. S14 is closed and the buret is again read with the solution in K2 at tip T2 as before. The pressure between R and B is equalized by opening S8 first, then S13, which allows the solution in K2 to drop from T2 to a level equal to that in B. The flow of nitrogen used to stir the solution in R is not interrupted during either of these transfer operations.

The polysulfides form very slowly and, on the scale of operation used in the present work, complete dissolution of the sulfur required as much as 12 hr. All of the alkali polysulfide solutions are red in color and appear to be perfectly homogeneous.

Upon completion of the interaction of alkali metal and sulfur, reference electrode E_r is introduced by first turning off the nitrogen stream used to stir the contents of R, placing S8 in position 1,3, and then turning S7 to position 1,3 and removing the plug from J4 of Fig. 1. E_r is quickly transferred from J (Fig. 2*b*) to J4 (Fig. 1), whereupon the condensation of the gaseous ammonia in compartment C (Fig. 2*a*) of electrode E_r causes this compartment to become filled with polysulfide solution from R via capillary K. S7 and S8 are returned to position 1,2 and the stirring of the contents of R by nitrogen gas is resumed.

The titration is conducted in conventional manner by transferring small portions of alkali metal solution from B to R by the procedure already described, and measuring the potential after each addition. In this work, very small portions (usually around 0.3 ml) were added and every precaution was taken to insure the re-establishment of equilibrium before potentiometer readings were recorded. In some cases this required only a few minutes; in others, as much as one hour was required for constant potentiometer readings after each addition of alkali metal solution.

[8] O is a short section of rubber tubing inside of which is a wire and which is nearly closed by a pinch clamp whereby the rate of air flowing through the rubber tubing and hence through S14 is controlled.

Experimental Results

All potentiometric titrations reported in this paper were carried out at $-38° \pm 0.5°C$. Alkali polysulfides having compositions within the range M_2S_{12} to M_2S_6 (where M = Na, K, Rb, or Cs) were prepared *in*

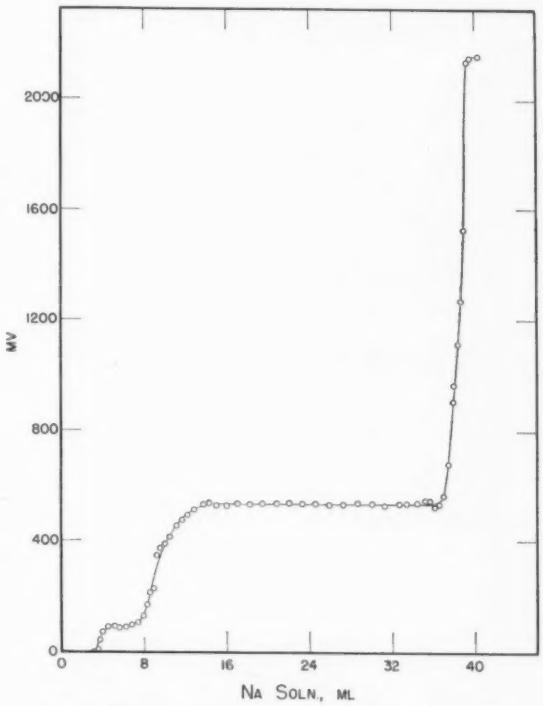

FIG. 3. Titration of sodium polysulfide with sodium

situ in the presence of the corresponding alkali iodides and titrated with standard solutions of the corresponding alkali metals. A feature common to all of these titrations was an initial rise in potential amounting to approximately 100 mv; this was observed regardless of the initial composition of the solution titrated. In all cases the formation of a precipitate was observed just past the M_2S_4 inflection point. The time required for the actual potentiometric titrations ranged from 25 to 40 hours.

Essential data relative to typical experiments are given in Table I; the actual titration data are shown graphically in Fig. 3 to 7, inclusive. Fig. 5 represents a case that differs from the others in that it involves the titration of *potassium* polysulfide with potassium

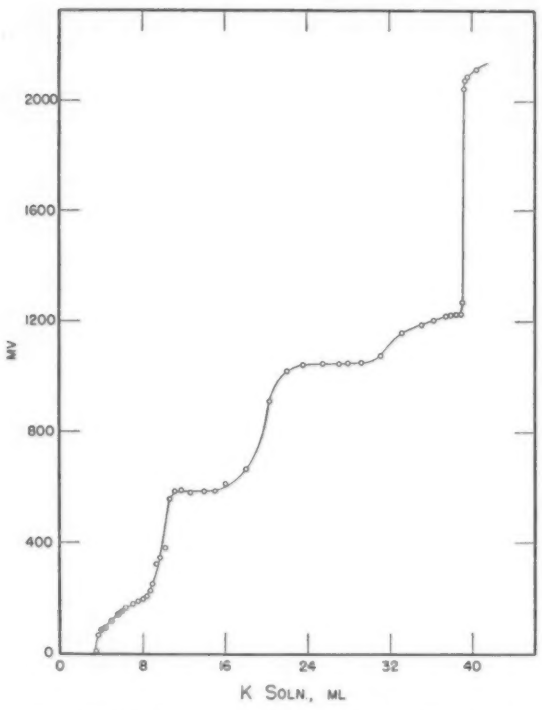

FIG. 4. Titration of potassium polysulfide with potassium (in the presence of potassium iodide).

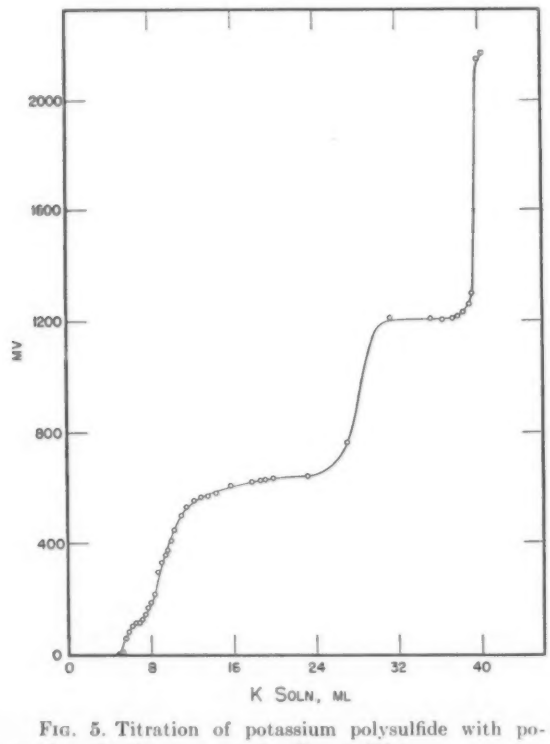

FIG. 5. Titration of potassium polysulfide with potassium (in the presence of sodium iodide).

in the presence of *sodium* iodide. In Table I, the inflection points and the change in potential, ΔV, were obtained graphically from the titration curves shown in Fig. 3 to 7.

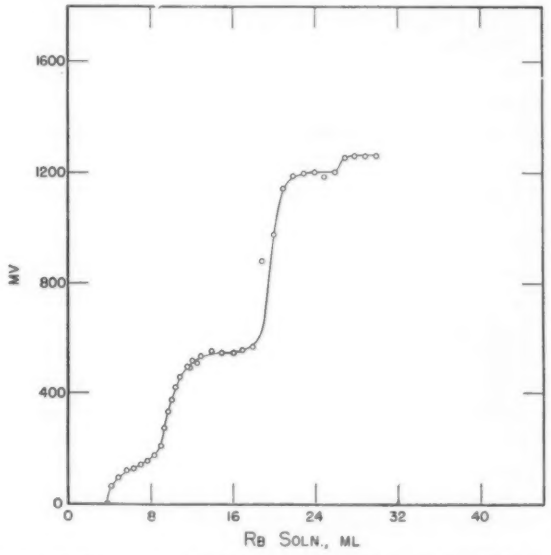

FIG. 6. Titration of rubidium polysulfide with rubidium

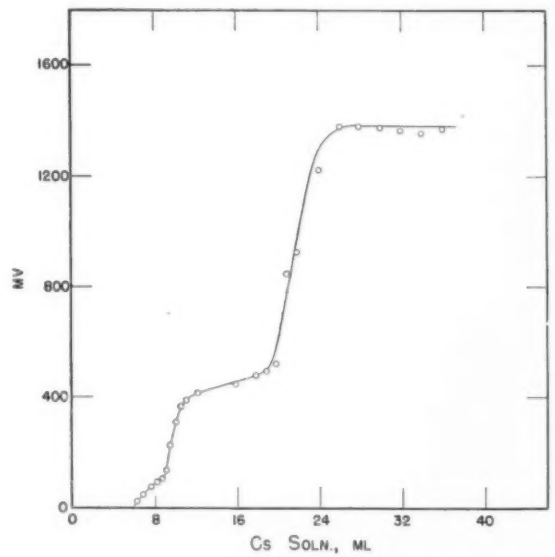

FIG. 7. Titration of cesium polysulfide with cesium

DISCUSSION

The data represented by Fig. 3 show clearly the formation of the compounds Na_2S_4 and Na_2S. On the basis of his studies of reactions carried out at $-33°$ C in a manner just the reverse of the procedure employed in the present work (i.e., addition of sulfur to ammonia solutions of sodium to form Na_2S, fol-

lowed by further additions of sulfur), Bergstrom (5) reported the formation of Na_2S, Na_2S_2, and Na_2S_4, but indicated that considerable difficulty was encountered in detecting end-points. The fact that the present work provided no evidence whatever for the formation of Na_2S_2, together with a careful inspection of Bergstrom's published data, suggests that the composition attributed to Na_2S_2 may have been a mixture of Na_2S and Na_2S_4. Through the use of methods quite similar to those employed in the present investigation, but involving titrations at −60°C, Zintl and co-workers (1) found evidence for the formation of Na_2S_6, Na_2S_5, Na_2S_4, Na_2S_3, Na_2S_2, and Na_2S. However, only the inflection points corresponding to Na_2S_6, Na_2S_4, and Na_2S were reproducible, and this fact was clearly brought out by Zintl, *et al.*, but has apparently been overlooked by others (6). Since the present work confirms the formation of Na_2S_4 and Na_2S, there remains the question relative to Na_2S_6, and the broader question of the existence—in ammonia—of polysulfides of the type $Na_2S_{>4}$.

It has already been pointed out that, in the present work, each titration showed an initial rise in potential amounting to approximately 100 mv *regardless of the initial composition*. In most of their titrations, Zintl and co-workers used initial polysulfide compositions approximating Na_2S_6; hence it is not surprising that their first observed change in potential was erroneously attributed to this particular species. It is our opinion that the initial polysulfide solutions of high sulfur content consist of a species that is the precursor of Na_2S_4 together and in equilibrium with sulfur in solution in liquid ammonia. It is well known that sulfur exhibits appreciable solubility in ammonia and that it reacts at least to a limited extent to form "derivatives of ammonium sulfide and sulfur nitride" (7). At least on a qualitative basis, the results of the present work are consistent with the view that the initial 100-mv change may be attributable to the conversion of dissolved excess sulfur or the products of its interaction with the solvent to that species which is the precursor of Na_2S_4. Finally, it should be recognized that Hugot (8) has reported the formation of Na_2S_5 by the direct interaction of sodium and sulfur in liquid ammonia; however, Bergstrom (5) attributes this result to failure to attain equilibrium.

Table I. *Data relative to the potentiometric titration of alkali polysulfides with alkali metals in liquid ammonia at −38°C*

Fig. No.	Soln. titrated[a]		Normality of metal soln.	Inflection point			Sulfur/metal	
	Sulfide[b]	MI, mg		Metal soln., ml	Approx. ΔV, mv	Compound indicated	Calcd.	Found
3	Na_2S_{12}	100.6	0.0534	9.2	440	Na_2S_4	2.0	2.1
				38.9	1620	Na_2S	0.50	0.50
4	K_2S_{11}	111.1	0.0516	10.0	355	K_2S_4	2.0	1.9
				20.0	455	K_2S_2	1.0	0.95
				39.2	860	K_2S	0.50	0.49
5	K_2S_8	100.5[c]	0.0443	9.2	440	K_2S_4	2.0	2.1
				28.5	550	M_6S_4[d]	0.67	0.67
				39.6	950		0.50	0.49
6	Rb_2S_{10}	142.6	0.0663	10.0	340	Rb_2S_4	2.0	1.9
				19.8	640	Rb_2S_2	1.0	0.95
7	Cs_2S_6	173.2	0.0410	9.7	255	Cs_2S_4	2.0	2.0
				21.8	870	Cs_2S_2	1.0	0.89

[a] The approximate volume of each initial sulfide solution was 45 ml.
[b] Approximate composition assuming complete interaction of sulfur and metal (see DISCUSSION).
[c] Sodium iodide.
[d] Where M = K and/or Na.

The data shown in Fig. 4 are entirely in agreement with results obtained earlier by Bergstrom (5) and show unequivocally the formation of K_2S_4, K_2S_2, and K_2S. The slight increase in potential which occurs after addition of approximately 30 ml of potassium solution does not correspond to any reasonable composition. It is of particular interest to observe, by comparison of Fig. 4 and 5, that different results are obtained when sodium iodide is substituted for potassium iodide in the titration of potassium polysulfide with potassium. In the presence of sodium iodide, there is no end-point corresponding to K_2S_2 but there is formed a compound corresponding to the formula M_6S_4. This result, as well as the absence of K_2S_2, could well arise because of altered solubility relationships owing to the presence of sodium ion.

The formation of mixed alkali metal salts in liquid ammonia has been reported previously (9), and it seems likely that the compound M_6S_4 is of this type.

As shown in Fig. 6 and 7, both rubidium and cesium polysulfides are converted successively to the tetrasulfides and disulfides when titrated with solutions of the corresponding metals. It proved impractical to continue these titrations to the monosulfide end-points because the dense yellow crystals of the apparently quite insoluble disulfides reacted so slowly with metal solutions that several hours were required for completion of the reaction with 1-ml portions. Klemm and co-workers (10) have prepared the monosulfides of rubidium and cesium by the direct interaction of the elements in liquid ammonia.

Summary

Relatively simple apparatus and procedures for carrying out potentiometric titrations in liquid ammonia have been developed and described in detail. The utility of these methods has been demonstrated in studies involving the titration of liquid ammonia solutions of alkali polysulfides with liquid ammonia solutions of alkali metals.

It has been shown that polysulfides of sodium, potassium, rubidium, and cesium react with solutions of the corresponding metals to form salts of the type M_2S_4 in all cases, M_2S_2 in the cases of potassium, rubidium, and cesium, and M_2S in the cases of sodium and potassium. No evidence for the existence of several sulfides of sodium previously reported as products of similar reactions could be obtained.

Any discussion of this paper will appear in a Discussion Section, to be published in the December 1951 issue of the Journal.

References

1. E. Zintl, J. Goubeau, and W. Dullenkopf, *Z. physik. Chem.*, **A154,** 1 (1931).
2. G. W. Watt, *Chem. Revs.*, **46,** 289, 317 (1950).
3. W. C. Johnson and W. C. Fernelius, *J. Chem. Education*, **6,** 441 (1929).
4. E. Muller, *Z. physik. Chem.*, **135,** 102 (1928).
5. F. W. Bergstrom, *J. Am. Chem. Soc.*, **48,** 146 (1926).
6. H. J. Emeleus and J. S. Anderson, "Modern Aspects of Inorganic Chemistry," p. 448, D. Van Nostrand Company, New York (1939).
7. O. Ruff and E. Geisel, *Ber.*, **38,** 2659 (1905).
8. C. Hugot, *Compt. rend.*, **129,** 299 (1899).
9. E. B. Maxted, *J. Chem. Soc.*, **111,** 1016 (1917).
10. W. Klemm, H. Sodomann, and P. Langmesser, *Z. anorg. u. allgem. Chem.*, **241,** 281 (1939).

The Structure of Metal Deposits Obtained by Electrochemical Displacement upon Zinc[1]

M. E. Straumanis and C. C. Fang

Department of Metallurgy, University of Missouri School of Mines and Metallurgy, Rolla, Missouri

ABSTRACT

An attempt is made to identify the composition and the structure of nonadherent immersion deposits of noble metals on zinc. For this purpose Cu, Au, Ni, and Ag deposits, obtained by electrochemical displacement from their salt solutions in 1*N* sulfuric acid, were examined by x-rays. All of them contained redeposited Zn. Cu deposits contained approximately 9 to 13 atom per cent in solid solution, and Ni deposits contained 17 to 20 per cent in solid solution; Au deposits large amounts and Ag deposits below 0.5 atom per cent. The grain size of the deposits was very small because their growth was hampered by codeposited Zn. During the displacement of Ag, zinc deposited mostly as a very thin layer on the surface of the grains. The other three metals absorbed Zn readily, forming α-phases. The displacement of the noble metal occurs because of the activity of the local cells; Zn acts as anode and the noble metal forms very small cathodes. The redeposition of Zn on these cathodes is possible because it is deposited in form of a solid solution, the free energy of which is reduced.

Introduction

Highest purity zinc dissolves very slowly in dilute acids (1*N* to 4*N* hydrochloric or sulfuric acid) (1). On adding to the solution a small amount of a salt from which a metal with low overvoltage can be displaced upon the zinc, the rate of dissolution is increased greatly (2). Not all metals more noble than Zn increase its dissolution rate in the same order as their hydrogen overvoltages decrease (3). Among the exceptions are Cu, Au, and especially Ag. A large increase in the rate of dissolution of Zn might be expected for Ag since it has a low overvoltage. However, this is not realized. It was suspected that the small effect of the dark deposits of Ag (also of Cu and Au) thus formed on Zn (4) might be caused by coprecipitated Zn which exhibited a high overvoltage. Indeed, Mylius and Fromm could show that Ag and Cu displaced from neutral solutions on Zn contained up to 50 per cent of Zn (5).

The intention of the present paper is to prove that even in acid solutions the deposits of Cu, Au, Ni, and Ag contain Zn and that, therefore, the assumption of a high overvoltage on these deposits is justified. Further, the structure of the deposits and their grain growth are discussed in connection with the x-ray photographs obtained.

[1] Manuscript received June 7, 1950. Based on a thesis submitted by C. C. Fang in partial fulfillment of the requirements for the Master's degree to the Graduate School, School of Mines and Metallurgy, The University of Missouri. This paper prepared for delivery before the Washington Meeting, April 8 to 11, 1951.

The question of the structure of the deposits produced by electrochemical displacement is now of some importance, as propositions have been made to cover metals with more noble ones using this process [Fe with Ni (6, 7) Al with Zn, Cd, Sn (8)]. No references concerning x-ray investigation of such metallic deposits could be found in the literature.

Experimental Procedure

The following operations were used in all tests to obtain the deposits, separate them from Zn, and to prepare them for the further investigation:

(1) A piece of C.P. Zn rod was treated for 15 to 30 seconds in 1.42 sp gr nitric acid to remove all sharp edges; it was then washed in distilled water and introduced into a test tube containing 3 ml of 2*N* sulfuric acid; 3 ml of a 0.1*M* salt solution of the metal in question were added to this giving a 1*N* acid solution.

(2) After the deposit had formed in an amount sufficient for further experiment (in 5 to 30 minutes), the tube was shaken to separate the deposit from the Zn. The solution was then quickly poured off and the precipitate washed in distilled water. Removal of the acid prevented the dissolution of Zn which otherwise might be distributed in the deposit of the nobler metal. Several decantations of the deposit with distilled water and tests for SO_4^{--} (with $BaCl_2$) followed to assure that the deposits did not contain soluble substances, e.g. $ZnSO_4$.

(3) Finally, the wet Ag deposits were washed

with alcohol and dried at room temperature, while the others were dried by gentle heating at approximately 50°C.

To study each deposit, the sample was divided into three parts:

(*a*) An x-ray photograph of the dark, dry deposit was made.

(*b*) One part of the precipitate was treated for a prolonged time with acid and the residue was analysed by x-rays. The presence of Zn^{++} in the acid solution after this treatment was confirmed.

(*c*) To determine quantitatively the amount of Zn present, the deposit was put into a narrow-necked quartz tube which was evacuated, sealed, and heated to 800°–900°C to homogenize the powder. As no reducing agents were present in the powder (the filtration of the deposits was also omitted in order not to contaminate them with filter paper fibers), reduction processes could not occur during annealing. If a trace of $ZnSO_4$ were still present it would be converted into ZnO and SO_3 which would not be reduced by the noble deposit. Thus, any Zn present would have had to come by co-deposition. The homogenized powders were used to obtain x-ray patterns. The films were measured and the lattice constants computed. From these data it was possible to determine the total Zn content of the deposits. The method is sufficiently precise (9) so that there was no need for quantitative chemical analyses, for which the amount available was too small. The photographs for comparison and for determination of the lattice parameters were made by the asymmetric method (10). A minus 400-mesh sample of the powder was attached with Cello-Seal[2] to a practically nonabsorbing Li-B-glass hair of 0.08–0.12 mm diameter. The powder mount had a diameter of about 0.18 mm. For such a tiny sample, the corrections due to absorption by the specimen were reduced to a minimum, using the last lines in the back-reflection region for the parameter calculations. Therefore, no absorption corrections were applied (11).

All metals and chemicals used were of highest purity available.

Experimental Results

Displacement of copper.—Using a 0.1*M* $CuSO_4$ solution a dark red, spongy deposit appeared on the Zn. When washed, dried, and examined under the microscope, the deposit was still dark red with some particles of faint red and yellow brass color. If the powder was rubbed or ground the color of brass was unmistakable.

The precipitate that peeled off the Zn piece during deposition gradually became copper-red in the acid solution and, simultaneously, a slight evolution of gas (hydrogen) could be observed on the surface of the precipitate. The same was true when the dry powder was treated with hydrochloric acid. Zn was identified in the solution by qualitative analysis (12).

The x-ray patterns of the dark Cu deposits differed from that of pure Cu (Fig. 1*a*) and were not the same in all experiments. The last lines, (331) and (420), were broad, faint, and considerably shifted from their old positions, especially when $ZnSO_4$ was added to the solution, indicating very fine grain size and lattice expansion.

The dark Cu deposit treated with cold 2*N* sulfuric acid gave an x-ray pattern of broad lines of nearly the same lattice parameter as pure Cu, but the inner edges of the last lines were sharper (Fig. 1*c*), indicating that part of the Zn was already dissolved. When the deposits were boiled in 2*N* sulfuric acid or treated with the cold acid for several days, the lines appeared normal again except that they remained broad.

The dark deposits, when heated in vacuum, turned yellow. The copper lattice simultaneously expanded still more in most cases because of the dissolution of particles rich in Zn, which had formed on separate points of the deposits and which were not always indicated by the x-ray patterns. The lines became sharper, due to increase in grain size and to more even distribution of Zn throughout the deposit. The Zn diffusion process, therefore, was completed at elevated temperatures, α-brass was formed, and an increase in the Zn content was observed after heating (Fig. 1*d*). In Table I are shown the lattice constants obtained with different Cu deposits and the computed Zn content using previously published α-brass x-ray data (14). The accuracy of determination for the case of sharp lines was ± 0.0008 kX (Fig. 1*a* and *d*), and for the case of broad lines it was only ± 0.002 kX. Nevertheless, the picture and the tabulated data show unmistakably the expansion of the lattice, caused by the dissolution of appreciable amounts of metallic Zn in the deposited Cu.

Displacement of gold and nickel.—For the displacement of gold by zinc, a $HAuCl_4$ solution was used. The reaction proceeded rapidly. The x-ray pictures showed that the grain size of the Au deposits was very small (10^{-5} to 10^{-6} cm) and that they contained Zn in solid solution (contraction of the Au lattice) (15). If annealed, a new phase was formed beyond the α-region of the solid solution Au-Zn, indicating that large amounts of Zn were absorbed by the gold deposit.

[2] Fisher Scientific Company, Pittsburgh, Pennsylvania.

The Zn from the dark deposits could be removed quickly only by boiling in nitric acid. Sulfuric acid acted very slowly. No recrystallization of the deposit took place at room temperature.

The process of the displacement of Au on Zn proceeds, therefore, in the same manner as in the case of Cu.

However, the lattice constant was the same as that of pure silver. The dark deposits turned white after annealing in vacuum. The x-ray pictures of the white deposits were sharp and the lattice constants nearly the same as for pure Ag. The black silver deposit contained small quantities of Zn since: (*a*) in sulfuric acid the deposit evolved small amounts of hydrogen and turned white (the x-ray pictures showed that the deposit had recrystallized); (*b*) the presence of Zn^{++} was detected in the solution just mentioned (12) but not in blank tests; (*c*) darker deposits were obtained when the deposition occurred from sulfuric acid solutions containing $ZnSO_4$ originally. The process of Ag deposition was very similar to that of Cu deposition, except that zinc did not diffuse into silver at room temperature. The amount of

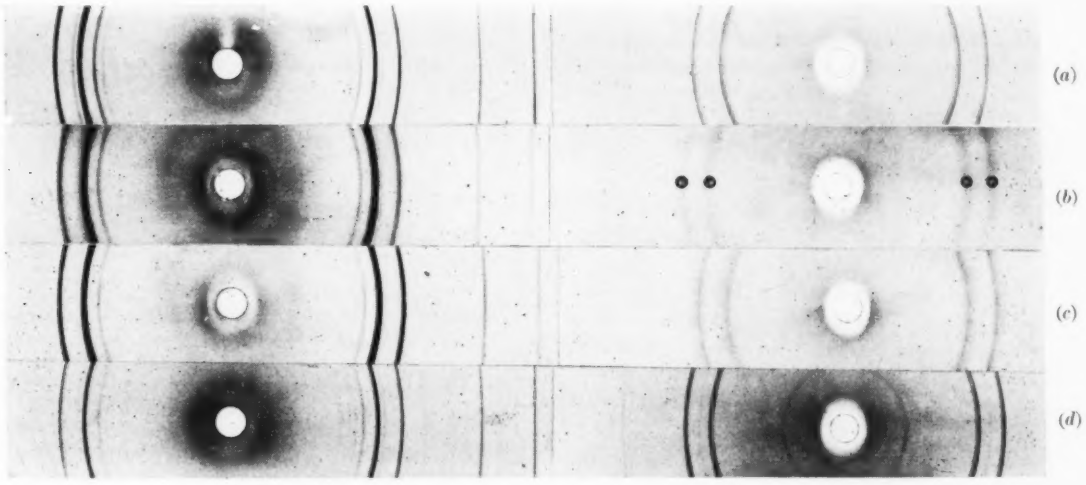

FIG. 1. X-ray patterns of Cu deposits obtained by electrochemical displacement on Zn. (*a*) pure Cu, (*b*) dark red Cu deposit (α-brass), (*c*) dark deposit treated with sulfuric acid, (*d*) dark deposit annealed in vacuum to 800°–900°C (α-brass).

The same is true concerning Ni deposits. The grayish black deposit of Ni on Zn, obtained from a $NiSO_4$ solution, could be separated from Zn only with difficulty, and it showed an x-ray pattern without back reflection lines. Even the front reflections were broad indicating a very small grain size (approximately 10^{-6} cm). The deposit could be dissolved entirely in cold $2N$ sulfuric acid in 10 minutes. Annealed in vacuum, a new phase was formed, showing the presence of large amounts of Zn in the deposit (approximately 17–20 atom per cent).

Displacement of silver.—The formation of the silver deposit using $0.1M$ $AgNO_3$ differs in some respects from the previous three cases. The deposit on the Zn grew to a velvety black sponge and occasionally black sponge particles were detached from the Zn surface by hydrogen bubbles. These particles changed color from black to white. This same effect was achieved by treating the sponge with $2N$ sulfuric acid solution, which action was accompanied by slight liberation of hydrogen. A much darker sponge resulted if $ZnSO_4$ was initially added to the solution. In the dry state the deposit aggregates to particles, the outside of which are darker than the inside.

The x-ray picture of the black silver deposit showed the pure silver pattern but with broad lines. The grain size of such silver is, therefore, very small.

TABLE I. *Lattice constants and composition of different copper deposits*

Cu-radiation; the line 420 was used for the measurements. Room temperature.

Copper	Annealing		in kX	Atom % Zinc
	Temp °C	Time hr		
Pure	—	—	3.6075	—
Dark red	—	—	3.629*	10
Dark red	—	—	3.625*	9
Dark red → red**	—	—	3.608*	—
Dark red‡	—	—	3.635*	13
Dark red → yellow	788	1	3.6490	19.2
Dark red → yellow	900	3	3.6536	21.4

* Rough measurements of marked points.

** Treated with H_2SO_4.

‡ Deposited in the presence of $2M$ $ZnSO_4$ solution.

Zn present in the Ag deposit, therefore, must be small, below 0.5 atom per cent, corresponding to the error limit of determination (±0.0008 kX for the sharp lines of the heated deposits) (13).

Discussion

There are at least two possible explanations for the presence of Zn in the noble metals:

(1) The metallic Zn could be present in the deposit as fragments or as very small particles which were undermined and then separated from the original metal by the dissolution process.

(2) Zn could be redeposited in form of a solid solution together with the nobler metal by the emf of Zn itself.

If Zn particles were left in the deposits mechanically, the x-ray patterns of the unheated deposits would have shown separate Zn lines, unevenly blackened (because the quantity of the separated grains could not be large). Such lines could not be observed. The only Zn lines, sometimes present on a film, were faint and very uniform, indicating that the particle size of Zn was very small. Even if small, discrete zinc particles were present, the formation of a Zn-Cu solid solution would require a different explanation because even colloidal Zn in contact with solid Cu would not dissolve at room temperature. Since the presence of solid solutions was proved in all Cu-, Au-, or Ni-deposits by the x-ray, the second mechanism seems more probable.

The Displacement Process

In order to understand the Zn redeposition achieved by the emf of Zn itself, the electrochemical displacement upon Zn must be considered first.

According to observations, the precipitation of the nobler metal starts on discrete points of the Zn surface, where there are evidently some discontinuities. If the first nuclei, consisting of the nobler metal, are formed, the precipitation then continues from these nuclei as starting points, because this growth requires less energy than the formation of new nuclei (16, 17). A Cu particle grows simply by cathodic deposition. Zn acts as anode and after the deposit forms, it acts cathodically. The electrolyte contains not only sulfuric acid and sulfates, chlorides, or nitrates of the nobler metals but also Zn ion, especially in the limiting layer. A current is supplied by Zn that goes into solution and at a potential limited by that of Zn in 1*N* sulfuric acid (ca. −0.71 volts) (19). The electrons flow from the Zn piece into the Cu deposit. The potential of the cathode (Cu deposit) (18), ϵ_c, is given by the equation:

$$\epsilon_c = \epsilon_a + ir + \eta \qquad (I)$$

where ϵ_a is the anode potential, i the current in the particle of the noble metal, r its resistance, which can vary considerably in the different parts of the particle, causing different rates of deposition (see Fig. 2), and η the polarization due to the hydrogen discharge on the surface of the particle. This potential is

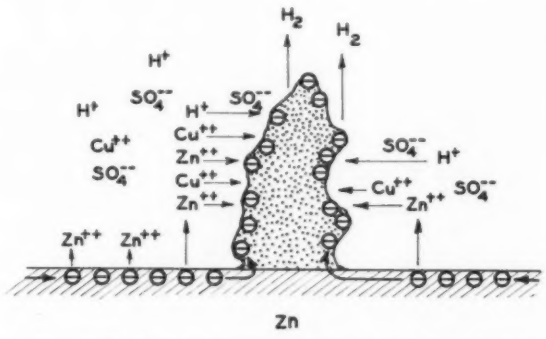

Fig. 2. Cu displaced upon Zn. The tiny Cu particle on the Zn surface acts as cathode; Cu^{++}, H^+, and finally a mixture of Cu^{++} and Zn^{++} are discharged on it. In the latter case a solid solution is formed.

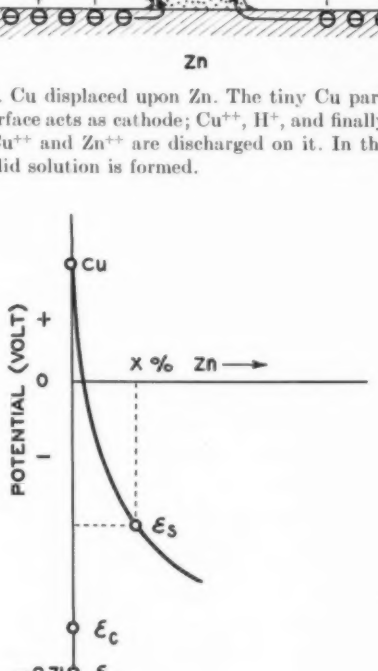

Fig. 3. Potential of a Cu-Zn solid solution versus per cent Zn. ϵ_a—dissolution potential of Zn (−0.71 volt), ϵ_c—potential of the Cu cathode (eq I), ϵ_s—potential required for desposition of a solid solution containing x per cent Zn.

quite insufficient to deposit Zn from the same solution, if the nature of the cathode is not considered.

It is well known that zinc forms solid solutions with copper and the reversible potential of a solid solution generally lies between those of the pure constituents (20, 22). Tammann (21) gives a formula for the potential of a solid solution, provided that it is in equilibrium with its ions and the diffusion in the solid

is rapid (25), as schematically represented by Fig. 3, showing the anodic and cathodic potentials of a local cell during the formation of a solid solution (containing Zn) by electrochemical displacement. The curve shows that the deposition potential of the solid solution ϵ_s is less anodic than that of the anode (Zn) and, therefore, Zn in solid solution can be deposited by the emf of Zn itself. The same relates also to the Au and Ni deposits (23, 24).

The codeposition of Zn hampers the growth of the deposits and, as a result, a very fine-grained deposit is obtained (17).

If the components do not form solid solutions, as is the case in the displacement of Pb^{++} or Cd^{++} by Zn, the deposits are pure and coarse crystalline, because the cathodic crystallization process is not disturbed by the discharge of Zn^{++}.

The process of Ag displacement is somewhat different. Although Ag forms solid solutions with Zn, only small amounts of Zn could be found in the deposits. It is believed that the low Zn content may be explained by the low rate of diffusion of Zn into Ag at room temperature and by the simultaneous action of the acid. The whole deposit consists, therefore, of tiny Ag particles (diameter approximately 10^{-5} cm) covered with a very thin Zn layer, not detectable by x-rays. The deposit has a black appearance because of the fine grain size. The deposit is fairly stable if it is in contact with Zn. If some black particles separate, the Zn on these particles dissolves quickly in the acid solution because the Ag acts as a large local cathode (contrary to the behavior of Cu- or Au-deposits under the same conditions). The silver grains grow even at room temperature and turn white (recrystallization, sharp x-ray pattern). In neutral solutions, such a dissolution is impossible and the Ag deposits show a high Zn content as already observed by Mylius and Fromm (5).

Since the noble metal deposits contain Zn in solid solution, and the Ag deposit has Zn on its surface, the hydrogen overvoltage of the deposits must be high. This confirms the assumption made earlier and explains the low activity of the deposits with respect to the dissolution of solid Zn in acids.

Acknowledgment

The authors wish to express their thanks and sincere appreciation to Dr. D. S. Eppelsheimer, Professor of Metallurgical Engineering, for his kindness in making available his x-ray unit; to Dr. H. R. Hanley, Professor Emeritus of Metallurgical Engineering, for the donation of a sample of highest purity zinc for this study; and to Professor A. Legsdin of the Department of Metallurgy for correcting the English of the present paper.

Any discussion of this paper will appear in a Discussion Section, to be published in the December 1951 issue of the Journal.

References

1. M. Centnerszwer and M. Straumanis, *Z. physik. Chem.*, **A167,** 421 (1933).
2. M. Centnerszwer and M. Straumanis, *Z. physik. Chem.*, **118,** 415 (1925).
3. M. Straumanis, *Z. physik. Chem.*, **129,** 380 (1927).
4. M. Centnerszwer and M. Straumanis, *Z. physik. Chem.*, **A156,** 28 (1931).
5. F. Mylius and O. Fromm, *Ber.*, **27,** 630 (1894). See also G. Tammann, "A Text Book of Metallography," p. 332, The Chemical Catalogue Company, Inc., New York (1925).
6. E. Wainer and W. J. Baldwin, *J. Am. Ceram. Soc.*, **28,** 317 (1945).
7. W. A. Wesley and H. R. Copson, *J. (and Trans.) Electrochem. Soc.*, **94,** 20 (1948).
8. S. Heiman, *J. (and Trans.) Electrochem. Soc.*, **95,** 205 (1949).
9. M. E. Straumanis, *J. Am. Chem. Soc.*, **71,** 679 (1949).
10. M. Straumanis and A. Ievins, "Die Präzisionsbestimmung von Gitterkonstanten nach der asymmetrischen Methode," J. Springer, Berlin (1940); reprinted by J. W. Edwards, Ann Arbor, Michigan (1948).
11. M. E. Straumanis, *J. Applied Phys.*, **20,** 726 (1946).
12. W. Stahl and M. Straumanis, *Z. anal. Chem.*, **128,** 60 (1947).
13. H. Lipson, N. J. Petch, and D. Stockdale, *J. Inst. Metals*, **67,** 79 (1941).
14. W. Hume-Rothery, G. W. Lewin, and P. W. Reynolds, *Proc. Roy. Soc. London*, **157A,** 167 (1936).
15. E. A. Owen and E. A. O. Roberts, *J. Inst. Metals*, **71,** 213 (1945).
16. W. Blum and H. S. Rawdon, Jr., *Trans. Electrochem. Soc.*, **44,** 397 (1923); also F. Foerster, *Z. Elektrochem.*, **32,** 525 (1926).
17. W. Pfanhauser, "Galvanotechnik," p. 47, Akademische Verlagsgesellschaft, Leipzig (1941).
18. U. R. Evans, "Metallic Corrosion, Passivity and Protection," p. XXXIV, 257, 343, Edward Arnold and Co., New York and London (1948).
19. M. Straumanis, *Acta Univ. Latviensis*, **20,** 335 (1928).
20. S. Glasstone, "An Introduction to Electrochemistry," p. 488–489, D. Van Nostrand, Inc., New York (1942).
21. G. Tammann, "A Text Book of Metallography," p. 333, The Chemical Catalogue Company, Inc., New York (1925).
22. H. J. Creighton, "Principles and Applications of Electrochemistry," John Wiley & Sons, Inc., Vol. I, p. 264, New York (1943).
23. E. P. Schoch and A. Hirsch, *J. Am. Chem. Soc.*, **29,** 314 (1907).
24. F. Foerster, *Z. Elektrochem.*, **17,** 883 (1911); **22,** 85 (1916).
25. A. Ölander, *Z. Metallkunde*, **29,** 361 (1937).

The Effect of Acoustical Radiations on the Hydrogen Electrode[1,2]

ERNEST YEAGER AND FRANK HOVORKA

Department of Chemistry, Western Reserve University, Cleveland, Ohio

ABSTRACT

Mathematical consideration is given to the production of alternating components in the electrode potential of a hydrogen electrode in an acoustical field. The effect is discussed in terms of (*a*) a low-frequency region in which the instantaneous conditions are characterized as reversible and (*b*) a higher-frequency region in which relaxation phenomena result because of the lack of instantaneous equilibrium conditions. While the former case involves the use of thermodynamics, the latter requires a kinetic treatment. An attempt is made to relate the reaction constants for the processes at both the reversible and polarized hydrogen electrodes to the phase angle and amplitude of the effect throughout a range of frequencies. The effect at high frequencies may provide an interesting test for theories of rate processes at gaseous electrodes.

On several occasions (1, 2), gas electrodes, particularly hydrogen electrodes, have been reported to be sensitive to acoustical radiations both at audio frequencies (1) and ultrasonic frequencies (2) in terms of an alternating component in the electrode potential. Inasmuch as the electrode potential of a gas electrode is a function of pressure and temperature, such an effect is not surprising. Limited theoretical speculation as to the nature of the effect has been presented by L. V. Nikitin (3) on the basis of electrokinetic phenomena and Frumkin's slow-discharge theory of hydrogen overvoltage (4) and by the authors (5) in terms of thermodynamics. Although the latter mode of calculation may be reasonable for the reversible hydrogen electrode at low frequencies, it is doubtful that, at even audio frequencies, instantaneous conditions at the electrode can be described as reversible or equilibrium; hence, the effect might be smaller than the value predicted on the basis of thermodynamics.

In the present paper the effect of acoustical radiations will be considered for the special case (Part I) of the reversible hydrogen electrode at low frequencies and for the general case (Part II) of the hydrogen electrode, either reversible or polarized, over a wide range of frequencies. The latter case involves a knowledge of the rate processes at a hydrogen electrode, and hence, should be of interest to the overvoltage theorist. The mathematical treatment of neither case can be considered as final inasmuch as the physical nature of the hydrogen electrode is rather obscure.

I. The Reversible Hydrogen Electrode at Low Frequencies

Consider a concentration cell consisting of two reversible hydrogen electrodes (platinized platinum) with only one electrode in an acoustical field:

$$\underset{P_g^0,\,T_g^0}{(\text{Pt-Pt})\ \text{H}_2} \mid \underset{P_1^0,\,T_1^0,\,a_1^0}{\text{H}^+} \parallel \underset{P_1,\,T_1,\,a_1}{\text{H}^+} \mid \underset{P_g,\,T_g}{\text{H}_2\ (\text{Pt-Pt})}$$

(reference half-cell) (acoustical half-cell)

The symbols associated with the reference electrode (pressure and temperature of the gas and liquid phases and the activity of the hydrogen ions) represent also the time-average of the corresponding variables for the electrode exposed to acoustical radiations. If the variation in the potential of this cell is assumed[3] to be caused entirely by temperature and pressure fluctuations in the gas phase of the acoustical half-cell and the approximation $\ln(1+x) = x$ for $x \ll 1$ is applied, the electromotive force of this cell is given[4] by the equation,

$$E = -\tfrac{1}{2}RT_g^0(P_g - P_g^0)/P_g^0F + \tfrac{1}{2}S_g(T_g - T_g^0)/F, \quad (1)$$

where S_g is the molar entropy of hydrogen gas, R is the gas constant, and F is the Faraday of electricity.

In the application of thermodynamics to this ef-

[1] Manuscript received May 19, 1950. This paper prepared for delivery before the Cleveland Meeting, April 19 to 22, 1950.

[2] This paper has been prepared in conjunction with an Office of Naval Research contract, on the application of ultrasonics to electrochemistry, at Western Reserve University (Contract No. N7 onr 47002, Project No. NR 051 162).

[3] The contributions to the effect from pressure and temperature variations in the liquid phase amount to less than 0.2% of the total effect for the special case.

[4] Details concerning the derivation of this equation from thermodynamics are presented in the earlier paper by the authors on the hydrogen electrode (5).

fect, the inherent assumption is made that molecular hydrogen gas is in equilibrium with the electroactive phase, i.e., an atomic phase. If the pressure changes in the gas phase are adiabatic, then by the second law of thermodynamics,

$$\left(\frac{\partial T}{\partial P}\right)_s = \frac{T}{C_p}\left(\frac{\partial V}{\partial T}\right)_p$$

and

$$T_g - T_g^0 \leqq \tfrac{1}{2}[RT_g^0/C_p][(P_g - P_g^0)/P_g^0], \qquad (2)$$

where C_p is the molar heat capacity of the gas phase at constant pressure. The value for the temperature change in eq (2) should be considered as a limiting value, however, for it is doubtful that the temperature variations in a gas phase with obviously small dimensions compared to the wavelength at low frequencies are adiabatic. The condition that equilibrium be maintained at every instant, at least to a first order approximation, appears hardly feasible for practical purposes unless the temperature of all phases at the electrode are essentially the same. Inasmuch as the temperature variations in the liquid phase are very small because of the low temperature coefficient of expansion for liquids, $(T_g - T_g^0)$ will be assumed negligible. Eq (1) then simplifies to

$$E = -\frac{RT_g^0}{2F}\left(\frac{\Delta P_g}{P_g^0}\right), \qquad (3)$$

where $\Delta P_g = P_g - P_g^0$.

If the pressure amplitude of the incident acoustical radiations in the liquid phase is represented by p, the excess acoustical pressure in the hypothetical gas phase of the acoustical half-cell is approximately[5]

$$\Delta P_g = p[\exp i(\omega t - \sigma_1 x) + \exp i(\omega t + \sigma_1 x)], \qquad (4)$$

where ω is the angular velocity and σ_1 is the propagation constant, ω/g_1, where g_1 is the velocity of sound in the liquid phase. If eq (3) and (4) are combined,

$$E = -\frac{RT_g^0}{2FP_g^0}p[\exp i(\omega t - \sigma_1 x) + \exp i(\omega t + \sigma_1 x)] \qquad (5)$$

or

$$E = -10^{-8}p[\exp i(\omega t - \sigma_1 x) + \exp i(\omega t + \sigma_1 x)]$$

for the case where p, the pressure amplitude, is in dynes/cm^2. For acoustical radiations with an intensity of one watt/cm^2, the amplitude of the alternating component in the electrode potential should be 10^{-2} volts.

[5] This equation is valid only for the case where the acoustical waves are total reflected for practical purposes at the surface of the platinum. The pressure amplitude is the same in both the liquid and gas phases if the latter is small in thickness (compared to the wavelength) because the boundary conditions include continuity of pressure between phases. Further details concerning the reflection of acoustical waves at electrodes are given at the end of the paper (Appendix).

II. General Treatment of the Hydrogen Electrode Effect

The electrode reaction for the acoustical half-cell indicated in Part I may be represented as the sum of the two steps:

$$e^- + H^+ \underset{k_3}{\overset{k_4}{\rightleftharpoons}} H\text{—Pt} \underset{k_2}{\overset{k_1}{\rightleftharpoons}} \tfrac{1}{2}H_2(\text{gas})$$

where the intermediate state involves the formation of atomic hydrogen adsorbed on the surface of a metal, e.g., platinum. The reaction constants k_1, k_2, k_3, and k_4 are defined in the present discussion by the equation

$$-\frac{d\tau}{dt} = k_1\tau^2 - k_2P(1-\theta)^2 + k_3\tau - k_4c(1-\theta), \qquad (6)$$

where τ represents the concentration of atomic hydrogen adsorbed on the surface of the electrode in moles per unit of actual surface area, P is the pressure of the hydrogen gas, θ is the fraction of the single active sites which are occupied on the metal surface, $(1-\theta)^2$ is a factor (6) representing the number of double active sites which are unoccupied, and c is the concentration of hydrogen ions in the electrical double layer (7). In eq (6) the interaction energy of neighboring hydrogen atoms adsorbed on the metal is assumed to be negligible.

In eq (6), k_1 and k_2 are essentially independent of the variables τ and P, although k_3 and k_4 may depend on τ and c since the energy of activation is a function of the absolute single electrode potential, ψ. The surface concentration of atomic hydrogen is proportional to θ, i.e., $\theta = \kappa\tau$, where $1/\kappa$ is the surface concentration with all active sites occupied. In the presence of a periodic perturbation, let the symbols $\Delta\tau$, ΔP, and $\Delta\psi$ be defined by the equations $\tau = \tau^0 + \Delta\tau$, $P = P^0 + \Delta P$, and $\psi = \psi^0 + \Delta\psi$, where τ^0, P^0, and ψ^0 are the time-average values for the surface concentration, gas pressure, and electrode potential (potential of the electrode relative to the solution), respectively, with the temperature[6] and the concentration of hydrogen ions in the electrical double layer assumed to be constant. The latter seems a reasonable approximation even in the presence of ultrasonic waves if one notes how small the variations in charge distribution are in solutions subjected to ultrasonic radiations [the Debye effect (2, 8)].

[6] Temperature variations at the electrode are assumed to have a negligible effect as in Part I.

The reaction constants k_3 and k_4 may be represented by the expressions

$$k_3 = k_3^0 \exp\left(\frac{\alpha F}{RT} \cdot \Delta\psi\right) \cong k_3^0\left(1 + \frac{\alpha F}{RT} \cdot \Delta\psi\right) \quad (7)$$

and

$$k_4 = k_4^0 \exp\left(-\frac{\beta F}{RT} \cdot \Delta\psi\right) \cong k_4^0\left(1 - \frac{\beta F}{RT} \cdot \Delta\chi\right), \quad (8)$$

where k_3^0 and k_4^0 are the reaction constants associated with the average conditions τ^0, P^0, and ψ^0, and α and β are the fractions of the absolute electrode potential which influence the activation energy for the ionization and discharge processes, respectively. In order for eq (7) and (8) to conform with the Nernst equation under equilibrium conditions, $(\alpha + \beta)$ must equal unity. If these equations are combined with eq (6) and k_1 and k_2 are replaced by k_1^0 and k_2^0 for purposes of symmetry, we have to a first order approximation,

$$-\frac{d(\Delta\tau)}{dt} = (B + C)(\Delta\tau) + D(\Delta P) + A(\Delta\psi), \quad (9)$$

where

$$A = \frac{F}{RT}[\alpha k_3^0\tau^0 + \beta c k_4^0(1 - \kappa\tau^0)], \quad (9a)$$

$$B = k_3^0 + k_4^0 c\kappa, \quad (9b)$$

$$C = 2[k_1^0\tau^0 + k_2^0 P^0\kappa - k_2^0\kappa^2\tau^0 P^0], \quad (9c)$$

and

$$D = -k_2^0(1 - \kappa\tau^0)^2, \quad (9d)$$

since

$$-\frac{d\tau^0}{dt} = k_1^0(\tau^0)^2 - k_2^0 P^0(1 - \kappa\tau^0)^2 + k_3^0\tau^0 - k_4^0 c(1 - \kappa\tau^0). \quad (10)$$

The quantity ΔP is given by the equation[5]

$$\Delta P = p[\exp i(\omega t - \sigma_1 x) + \exp i(\omega t + \sigma_1 x)]$$

as in Part I.

The solution of eq (9) requires a relationship between $\Delta\psi$ and $\Delta\tau$. The electrode and the solution may be considered as the plates of a condenser with an effective charge of Q at any instant; hence, $\chi\psi = Q$, where χ is the effective capacity of the condenser. As in the case of τ, P, and ψ, let $\chi = \chi^0 + \Delta\chi$ and $Q = Q^0 + \Delta Q$. It is apparent that $\Delta Q = F(\Delta\tau_{34})$ where F is the Faraday and $(\Delta\tau_{34})$ is the contribution to $\Delta\tau$ from the ionization and discharge processes. To a first order approximation

$$\frac{d(\Delta\tau_{34})}{dt} = \frac{\chi^0}{F} \cdot \frac{d(\Delta\psi)}{dt} + \frac{\psi^0}{F} \cdot \frac{d(\Delta\chi)}{dt} \quad (11)$$

If eq (11) is combined with eq (9),

$$\frac{d^2(\Delta\psi)}{dt^2} + \left(B + C + \frac{AF}{\chi^0}\right)\frac{d(\Delta\psi)}{dt} + \frac{ACF}{\chi^0}(\Delta\psi) - \frac{BDF}{\chi^0}(\Delta P) + \frac{\psi^0}{\chi^0}\frac{d^2(\Delta\chi)}{dt^2} + \frac{(B + C)\psi^0}{\chi^0} \cdot \frac{d(\Delta\chi)}{dt} = 0. \quad (12)$$

In order to solve eq (12), an explicit relation is required between $\Delta\chi$ (the perturbation in capacity) and time. The capacity[7] shall be assumed to vary inversely as the effective distance of separation between the electrode and the effective plane of charge on the solution side. Since this distance is a periodic function of displacement in the acoustical waves, $\Delta\chi$ may be expressed in the form

$$\Delta\chi = p[M_1 \exp i(\omega t - \sigma_1 x) + M_2 \exp i(\omega t + \sigma_1 x)], \quad (13)$$

where p is the pressure amplitude of the incident waves and M_1 and M_2 are complex constants.[5]

Only the steady-state solution is desired for eq (12); hence, the alternating component in the electrode potential is assumed to take the form

$$\Delta\psi = \xi_1 \exp i(\omega t - \sigma_1 x) + \xi_2 \exp i(\omega t + \sigma_1 x), \quad (14)$$

where ξ_1 and ξ_2 are complex coefficients. Eq (12) is satisfied by eq (14) when

$$\xi_1 = -\frac{BD + (\psi^0/F)M_1[\omega^2 - i(B + C)\omega]}{[(\chi^0\omega^2/F) - AC] - i[(B + C)(\chi^0/F) + A]\omega}\, p \quad (15)$$

and

$$\xi_2 = -\frac{BD + (\psi^0/F)M_2[\omega^2 - i(B + C)\omega]}{[(\chi^0\omega^2/F) - AC] - i[(B + C)(\chi^0/F) + A]\omega}\, p. \quad (16)$$

If L^0 represents the time-average value for the effective thickness of the dielectric of the condenser and ΔL the variation in this quantity as a result of the acoustical radiations, it can be shown that[5]

$$\Delta L \cong \frac{p}{i\omega}\left[\frac{R_d + R_m}{R_d(R_1 + R_m)}\right] \cdot [1 - \exp i(\sigma_d L^0)] \exp i(\omega t - \sigma_1 x) + \frac{p}{i\omega}\left[\frac{R_d - R_m}{R_d(R_1 + R_m)}\right] \cdot [1 - \exp i(-\sigma_d L^0)] \exp i(\omega t + \sigma_1 x), \quad (17)$$

where R_d, R_1, and R_m are the acoustical impedance (density × velocity) of the dielectric of the con-

[7] The nature of the dielectric of this condenser will be discussed at a later point in this paper.

denser, the solution, and the metal of the electrode, respectively, and σ_d is the propagation constant, i.e., ω/g_d, for the dielectric of the condenser. The variation in capacity is related to ΔL by the equation, $\Delta\chi = -(\chi^0/L^0)(\Delta L)$, which is applicable provided ΔL is small compared to L^0. Thus,

$$M_1 = \frac{i\chi^0}{L^0\omega} \cdot \frac{R_d + R_m}{R_d(R_1 + R_m)} [1 - \exp i(\sigma_d L^0)] \cong \frac{\chi^0}{g_d} \cdot \frac{R_d + R_m}{R_d(R_1 + R_m)} \tag{18}$$

and

$$M_2 = \frac{i\chi^0}{L^0\omega} \cdot \frac{R_d - R_m}{R_d(R_1 + R_m)} [1 - \exp i(-\sigma_d L^0)] \cong \frac{\chi^0}{g_d} \cdot \frac{R_m - R_d}{R_d(R_1 + R_m)}, \tag{19}$$

where M_1 and M_2 are both real numbers for practical purposes and independent of frequency, provided the dimension (L^0) of the condenser is small compared to the wavelength. The absolute values for ξ_1 and ξ_2 are

$$\xi_1 = \frac{BD}{AC}\left\{\frac{\left[1 + \frac{\psi^0 M_1\omega^2}{BDF}\right]^2 + \left[\frac{\psi^0 M_1\omega}{BDF}(B + C)\right]^2}{\left[1 - \frac{\chi^0\omega^2}{ACF}\right]^2 + \left[A + (B + C)\frac{\chi^0}{F}\right]^2\left(\frac{\omega}{AC}\right)^2}\right\}^{\frac{1}{2}} p \tag{20}$$

and

$$\xi_2 = \frac{BD}{AC}\left\{\frac{\left[1 + \frac{\psi^0 M_2\omega^2}{BDF}\right]^2 + \left[\frac{\psi^0 M_2\omega}{BDF}(B + C)\right]^2}{\left[1 - \frac{\chi^0\omega^2}{ACF}\right]^2 + \left[A + (B + C)\frac{\chi^0}{F}\right]^2\left(\frac{\omega}{AC}\right)^2}\right\}^{\frac{1}{2}} p \tag{21}$$

and the corresponding phase angles, δ_1 and δ_2 are

$$\delta_1 = -\arctan\frac{[A + (B + C)\chi^0/F]\omega}{AC - (\chi^0\omega^2/F)} - \arctan\frac{-\psi^0 M_1(B + C)\omega}{FBD + \psi^0 M_1\omega^2} \tag{22}$$

and

$$\delta_2 = -\arctan\frac{[A + (B + C)\chi^0/F]\omega}{AC - (\chi^0\omega^2/F)} - \arctan\frac{-\psi^0 M_2(B + C)\omega}{FBD + \psi^0 M_2\omega^2}. \tag{23}$$

If the electrode in the acoustical field is part of a cell of the type described in Part I, the electromotive force E of the cell will be identical with $\Delta\psi$, provided that the conditions of the reference electrode correspond to the average of the acoustical electrode; otherwise, $\Delta\psi$ represents the alternating component in E. In general, the average conditions represented by ψ^0, τ^0, and P^0 may be either reversible or irreversible. For the reversible case,

$$k_1^0(\tau^0)^2 = k_2^0 P^0(1 - \theta^0)^2 \tag{24}$$

and

$$k_3^0\tau^0 = k_4^0 c(1 - \theta^0). \tag{25}$$

Under these conditions, the alternating component is

$$\Delta\psi = -\frac{RT}{2P^0F}\left\{\frac{(1 - aM_1\omega^2)^2 + (bM_1\omega)^2}{(1 + r\omega^2)^2 + (s\omega)^2}\right\}^{\frac{1}{2}} \cdot p \exp i(\omega t - \sigma_1 x) - \frac{RT}{2P^0F}\left\{\frac{(1 - aM_2\omega^2)^2 + (bM_1\omega)^2}{(1 + r\omega^2)^2 + (s\omega)^2}\right\}^{\frac{1}{2}} \cdot p \exp i(\omega t + \sigma_1 x), \tag{26}$$

where

$$a = \frac{\psi^0(k_3^0 + k_4^0 c\kappa)}{k_2^0(k_3^0)^2F}, \tag{26a}$$

$$b = \left[\frac{\psi^0 P^0(k_3^0 + k_4^0 c\kappa)}{k_4^0 cF}\right]\left[\frac{2}{k_3^0} + \frac{k_3^0 + k_4^0 c\kappa}{k_1^0 k_4^0 c}\right], \tag{26b}$$

$$r = -\frac{\chi^0 RT(k_3^0 + k_4^0 c\kappa)}{2k_1^0(k_4^0)^2 c^2 F}, \tag{26c}$$

and

$$s = \frac{k_3^0}{2k_1^0 k_4^0 c} + \left[\frac{RT\chi^0}{2Fk_4^0 c}(k_3^0 + k_4^0 c\kappa)\right] \cdot \left[\frac{2}{k_3^0} + \frac{k_3^0 + k_4^0 c\kappa}{k_1^0 k_4^0 c}\right]. \tag{26d}$$

It should be noted that k_3^0, k_4^0, and ψ^0 are not independent of P^0 and c, since the electrode potential should follow the Nernst equation for reversible conditions. If ω is small, i.e., the effect observed at low frequencies, the alternating component will approach the value predicted earlier on the basis of thermodynamics:

$$\Delta\psi = -\frac{RT}{2P^0F}p[\exp i(\omega t - \sigma_1 x) + \exp i(\omega t + \sigma_1 x)].$$

If free hydrogen gas is not present at the electrode surface, an extremely small effect would be expected on the basis of thermodynamics except at very low frequencies when the concentration of hydrogen gas dissolved in the solution adjacent to the electrode might vary as a function of the pressure of the hy-

drogen gas in equilibrium with it. Experimental indications (1, 2) are that this view is correct. In the case of cathodically polarized electrodes, however, one would expect a hydrogen gas phase to form at the surface of the electrode if the surrounding solution has previously been saturated with hydrogen gas. Work in progress at Western Reserve University as well as previous work by Nikitin seems to confirm this conclusion. Acoustical effects have been observed at audio and ultrasonic (250 kc) frequencies with both cathodically and anodically polarized electrodes. Furthermore, on occasion, the acoustical sensitivity appears to persist for an appreciable time after cessation of the current. For the polarized hydrogen electrode, hydrogen gas is probably the dielectric of the condenser.

Eq (26) may be applicable to polarized electrodes when the current density is low and after the cessation of current. At higher current densities, however, eq (24) and (25) should be replaced by the expressions,

$$I = F[k_1^0(\tau^0)^2 - k_2^0 P^0(1 - \theta^0)^2] \qquad (27)$$

and

$$I = F[k_4^0 c(1 - \theta^0) - k_3^0 \tau^0], \qquad (28)$$

where I is the cathodic polarizing current. The reaction constants k_3^0 and k_4^0 may be related to the overvoltage η by the equations,

$$k_3^0 = {}_0k_3^0 \exp\left(-\frac{\alpha F}{RT}\eta\right) \qquad (29)$$

and

$$k_4^0 = {}_0k_4^0 \exp\left(\frac{\beta F}{RT}\eta\right), \qquad (30)$$

where ${}_0k_3^0$ and ${}_0k_4^0$ correspond effectively to the "reversible" values. For low frequencies, the capacitive effect, represented by terms involving M_1 and M_2 in eq (20) and (21), becomes small and the amplitude of the effect for the polarized electrode is

$$\xi_1 = \xi_2 = \frac{BD}{AC}p, \qquad (31)$$

where the terms A, B, C, and D depend on the polarizing current through eq (27–30).

For frequencies which are sufficiently high such that the internal impedance of the electrode is primarily capacitive, eq (20) and (21) become

$$\xi_1 = ({}_0\psi^0 - \eta)M_1 p/\chi^0 \qquad (32)$$

and

$$\xi_2 = ({}_0\psi^0 - \eta)M_2 p/\chi^0, \qquad (33)$$

where ${}_0\psi^0$ represents the reversible potential. Thus, at high frequencies, the gas electrode would be expected to act as a condenser microphone. Unfortunately, it is not possible to indicate what constitutes high and low frequencies as far as the effect is concerned since there is insufficient information on the rate processes at gas electrodes.

An attempt has been made in Fig. 1 to indicate the nature of the hydrogen electrode effect by an electrical diagram. In this diagram, the condenser C represents the capacity ($\chi^0 + \Delta\chi$) of the electrode to the solution, Z_{34} represents the equivalent electrical impedance associated with the rate constants k_3 and k_4, ψ is the d-c potential ψ^0 plus the alternating component $\Delta\psi$, and Z_s is the impedance associated with any rate processes in the electrical double layer and the solution, e.g., the resistance of the

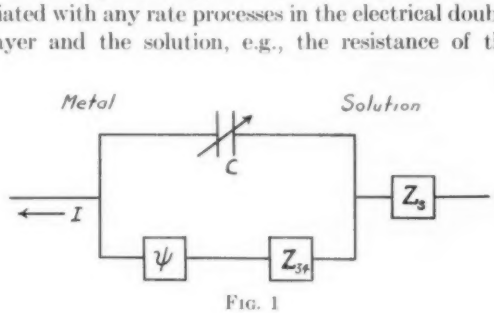

FIG. 1

solution. Z_{34} decreases as the frequency approaches zero.

In this treatment, the polarized electrode has been assumed to be surrounded by a more or less continuous film of gas. In practice, this is probably a poor assumption because the solution surrounding the electrode would be expected to wet the metal surface under most conditions. Thus, the continuous film should be replaced by a discontinuous phase consisting of a large number of closely spaced bubbles. If the surface conductivity of the solution is low, however, the concept of a leaky condenser should be a close approximation. If the effect is studied at appreciable polarizing currents, periodic fluctuations in bubble size as a result of the ultrasonic waves might produce a variation in the effective resistance to the flow of current at the electrode surface, and hence, an alternating component in the potential. In Fig. 1, this might be represented by a periodic variation in impedance Z_{34} as well as Z_s.

In the present discussion, any variation produced in the zeta potential by the acoustical waves has been assumed to be negligible. This seems reasonably justified in view of the fact that the reversible hydrogen electrode demonstrates little acoustical sensitivity.

The study of the effect of acoustical waves on the hydrogen as well as the oxygen electrodes should be interesting in terms of the fundamental nature of overvoltage. A detailed examination of the amplitude and phase angle of the effect as a function of frequency, extent of polarization, hydrostatic pressure, amplitude of acoustical waves, and concentration

of electrolytes should indicate the magnitude of the rate constants for the processes at the hydrogen electrode. The two steps cited above, while general, have been used primarily for the purpose of illustration. Any theory of overvoltage which is accepted in the future should be capable of explaining this effect quantitatively.

At the present time, the effect of ultrasonic radiations on the hydrogen electrode is under investigation at Western Reserve University in terms of both alternating components and uni-directional changes in electrode potential. The results of the experimental work on the a-c effect, which involves the use of pulse techniques, will be reported in the near future. One objective of the work, which is partially supported by an Office of Naval Research contract, is to ascertain the possibility of utilizing the hydrogen electrode as a hydrophone.

If the ideas expressed above are fundamentally correct, an inverse effect should be expected at a gas electrode; i.e., if an alternating potential is applied to a polarized electrode, a material wave of the same frequency should be generated in the solution surrounding the electrode. This remains to be confirmed experimentally.

APPENDIX

The Reflection and Transmission of Sound at a Gas Electrode

An electrode surface is represented in Fig. 2 with a dielectric d between the solution and the metal surface. In the present discussion the dimensions of the liquid and metal (platinum) phases will be considered infinite while the thickness L of the intermediate phase d is small compared to the wavelength. The subscripts 1, d, and m will be used with appropriate phases while j and k will indicate the phase boundaries (Fig. 2). The displacement in the liquid phase is

$$X_1 = A_1 \exp i(\omega t - \sigma_1 x) - B_1 \exp i(\omega t + \sigma_1 x) \quad (34)$$

where the first term represents the incident waves (traveling in the plus-x direction) and the second term represents the reflected waves. In addition, ω is the angular frequency of the waves, x is the distance in the direction of propagation, and σ_1 is the propagation constant ω/g_1 where g_1 is the velocity of the waves in the liquid phase. Likewise, the displacement in phase d and the metal are

$$X_d = A_d \exp i(\omega t - \sigma_d x) - B_d \exp i(\omega t + \sigma_d x) \quad (35)$$

and

$$X_m = A_m \exp i(\omega t - \sigma_m x). \quad (36)$$

From acoustical theory (9)

$$\Delta P = -\rho g^2 \frac{\partial X}{\partial x}, \quad (37)$$

where ρ is the density of the phase, ΔP the excess acoustical pressure, and g the velocity of sound. The boundary conditions include continuity of pressure between each phase and continuity of displacement normal to each boundary. If these conditions are applied in conjunction with eq (34–37) and the resulting four equations solved for B_1, A_d, and B_d in terms of A_1,

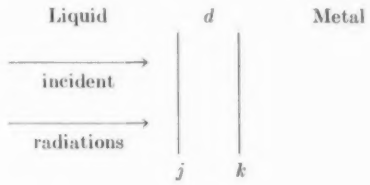

Fig. 2

$$B_1 = \frac{A_1}{U}[\exp i(\sigma_d L)][R_d^2 - R_d R_1 + R_d R_m - R_1 R_m] - \frac{A_1}{U}[\exp i(-\sigma_d L)][-R_d^2 - R_d R_1 + R_d R_m + R_1 R_m], \quad (38)$$

$$A_d = \frac{A_1}{U}[\exp i(\sigma_d L + \sigma_d x_j - \sigma_1 x_j)] \cdot [2R_1(R_d + R_m)], \quad (39)$$

and

$$B_d = \frac{A_1}{U}[\exp i(-\sigma_d L - \sigma_d x_j + \sigma_1 x_j)] \cdot [2R_1(R_m - R_d)], \quad (40)$$

where x_j represents the coordinates of boundary j and

$$U = [\exp i(\sigma_d L)][R_d^2 + R_d R_1 + R_d R_m + R_1 R_m] + [\exp i(-\sigma_d L)][-R_d^2 + R_d R_1 + R_d R_m - R_1 R_m], \quad (41)$$

where R_d, R_1, and R_m are the acoustical impedances (velocity × density) of the dielectric (e.g., hydrogen gas), solution, and metal.

Since the dimensions of the dielectric are small compared to the wavelength, terms involving only $\exp i(\sigma_d L)$ and $\exp i(-\sigma_d L)$ may be assumed equal to unity and terms involving $[1 - \exp i(\sigma_d L)]$ and $[1 - \exp i(-\sigma_d L)]$ may be assumed equal to $[-i \sin (\sigma_d L)]$ and $[+i \sin (\sigma_d L)]$, respectively.

If the excess acoustical pressure of the incident

waves in the liquid phase is

$$p[\exp i(\omega t - \sigma_1 x)] \tag{42}$$

then, by eq (37)

$$p = i\omega R_1 A_1. \tag{43}$$

The acoustical pressure in the liquid phase and the dielectric are essentially equal in view of the boundary conditions; hence,

$$\Delta P_d = \Delta P_1 = p\left[\exp i(\omega t - \sigma_1 x) + \frac{R_m - R_1}{R_m + R_1} \exp i(\omega t + \sigma_1 x)\right].$$

The specific acoustical resistance of platinum is approximately 6×10^6 cgs units while that of water is approximately 1.5×10^5; thus, for practical purposes,

$$\Delta P_d \cong p[\exp i(\omega t - \sigma_1 x) + \exp i(\omega t + \sigma_1 x)].$$

The difference between the displacements in the dielectric (hydrogen gas) at boundaries j and k is equal to the periodic change in the dimensions of the condenser. By the combination of eq (35), (39), and (40), ΔL is found to be approximately

$$\Delta L \cong \frac{p}{i\omega}\left\{\frac{R_d + R_m}{R_d(R_1 + R_m)}[1 - \exp i(\sigma_d L)] \cdot \exp i(\omega t - \sigma_1 x) + \frac{R_d - R_m}{R_d(R_1 + R_m)} \cdot [1 - \exp i(-\sigma_d L)] \exp i(\omega t + \sigma_1 x)\right\},$$

which is identical with eq (17) in Part II of this paper.

Any discussion of this paper will appear in a Discussion Section, to be published in the December 1951 issue of the JOURNAL.

REFERENCES

1. L. V. NIKITIN, *Compt. rend. acad. sci. U.R.S.S.*, **4,** 309 (1934); *J. Gen. Chem. U.S.S.R.*, **6,** 1393 (1936); *ibid.*, **6,** 1404 (1936); *ibid.*, **10,** 97 (1940); *ibid.*, **10,** 636 (1940). L. V. NIKITIN AND M. RAUSCH, *J. Phys. Chem. U.S.S.R.*, **20,** 325 (1946).
2. E. YEAGER, J. BUGOSH, F. HOVORKA, AND J. MCCARTHY, *J. Chem. Phys.*, **17,** 411 (1949).
3. L. V. NIKITIN, *J. Phys. Chem. U.S.S.R.*, **22,** 1096 (1948).
4. A. N. FRAMKIN, *Disc. Faraday Soc.*, **1,** 57 (1947).
5. E. YEAGER AND F. HOVORKA, *J. Chem. Phys.*, **17,** 417 (1949).
6. A. R. MILLER, "The Adsorption of Gases on Solids," pp. 70–77, Cambridge University Press, London (1949).
7. O. STERN, *Z. Elektrochem.*, **30,** 508 (1924).
8. P. DEBYE, *J. Chem. Phys.*, **1,** 13 (1933). J. BUGOSH, E. YEAGER, AND F. HOVORKA, *J. Chem. Phys.*, **15,** 952 (1947).
9. I. CRANDALL, "Theory of Vibrating Systems and Sound," p. 105, D. Van Nostrand Co., New York (1927).

The Formation of Molybdenum Disilicide Coatings on Molybdenum[1]

E. A. Beidler, C. F. Powell, I. E. Campbell

Battelle Memorial Institute, Columbus, Ohio

AND

L. F. Yntema

Fansteel Metallurgical Corporation, North Chicago, Illinois

ABSTRACT

Molybdenum can be rendered highly resistant to oxidation by treatment with a hydrogen-silicon tetrachloride atmosphere at 1000° to 1800°C so as to produce a molybdenum disilicide coating at its surface. Coatings 0.025 mm thick, thus produced, have completely protected the base metal for over 4000 hours in air at 1000°C, and for over 30 hours at 1700°C. Thicker coatings, within limits, give proportionately longer lives. Although brittle at room temperatures, the coatings have limited ductility at a red heat.

Introduction

As developmental work on materials of construction for high-temperature service continues, it becomes increasingly apparent that no one material, or group of materials, will have all of the desired properties.

Ceramic materials such as oxides, frequently used because of their chemical stability, are difficult to fabricate, and for the most part have low resistance to mechanical and thermal shock. Metals are more readily fabricated and are resistant to mechanical and thermal shock, but, with the exception of the platinum group metals, are subject to oxidation at elevated temperatures.

The possibility of using a metal with a ceramic or quasi-ceramic coating appears to be a possible solution to the problem of producing a material for extreme high-temperature service. One of the most promising of such materials is siliconized molybdenum, i.e., molybdenum with a coating of molybdenum silicides.

Molybdenum may be siliconized by a variety of methods such as hot dipping, spraying, and heating in a silicon pack. However, one of the most effective methods is by treatment in a $SiCl_4$-H_2 atmosphere at 1000°–1600°C, frequently referred to as the vapor-deposition method.

This paper summarizes results of experimental work on the formation of molybdenum disilicide coatings on molybdenum by reaction of molybdenum with a $SiCl_4$-H_2 atmosphere.

[1] Manuscript received March 23, 1950. This paper prepared for delivery before the Cleveland Meeting, April 19 to 22, 1950.

Experimental Work

Materials

Molybdenum.—Most of the exploratory work in preparing and testing molybdenum silicide coatings has been done on 2-mm-diameter molybdenum wire produced by the Fansteel Metallurgical Corporation. However, sheet, rod, and tubing, as well as numerous fabricated articles, have been coated.

Silicon tetrachloride.—The C.P. grade, containing 99.8 per cent $SiCl_4$, was fractionated under hydrogen and distilled into the saturator used in the coating process.

Hydrogen.—Tank hydrogen, 99.8 per cent pure, was passed over copper turnings at 400° to 600°C, and then through $MgClO_4$ and P_2O_5 drying towers and a furnace containing magnesium metal chips at 600°C.

Apparatus

The apparatus shown in Fig. 1 was developed for coating a series of short, straight lengths of the molybdenum wire in rapid succession. It consisted of two identical, water-cooled stainless-steel end pieces, each having a close-fitting central hole to receive the wire sample, a mercury gland to seal the wire entrance and gas entrance and exit apertures. The coating chamber was a water-jacketed 30-mm Pyrex tube, sealed to the end plates by rubber O-rings held

in grooves in the plates. The end plates were connected to the secondary of a step-down transformer whose primary was operated from a 20-amp Variac, permitting close control of the wire temperature. From 200 to 250 amp were required to heat the 2-mm-diameter molybdenum wire to coating temperature. Short lengths of wire were used in most of the coating work, but long lengths could be coated by slowly drawing the wire through the apparatus.

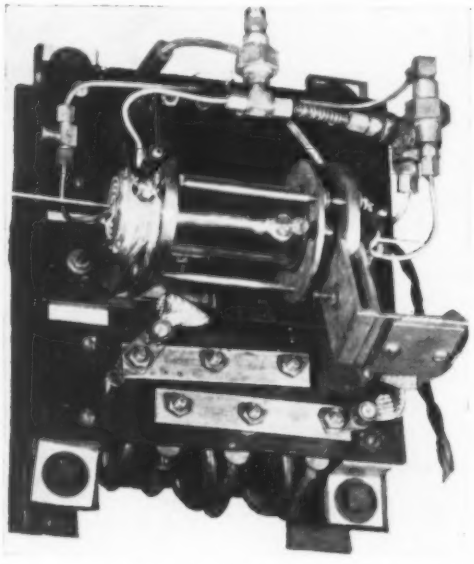

FIG. 1. Unit for siliconizing 2-mm-diameter molybdenum wire.

The coated wires were tested by heating them as resistors in air to the desired temperature and noting the time to failure. The wire was clamped horizontally in two heavy, water-cooled copper electrodes, one of which floated freely in a mercury well to allow expansion and contraction of the wire. The heating current was obtained from a step-down transformer fed by a 20-amp, 115-v Variac. A current transformer on one of the secondary leads activated a relay which closed the circuits to a time meter and to the Variac. Failure of the specimen opened the relay, shutting off the time meter. An auxiliary piece of equipment permitted the sample to be loaded for oxidation tests under tension.

Smaller molybdenum specimens (0.5-mm wire) were bent into loops and heated electrically for coating and testing. Larger objects, such as 6- to 12.5-mm-diameter tensile bars, were heated inductively or in externally heated furnaces, the former method being preferred.

Procedure

After inserting the cleaned specimen in the coating chamber, the chamber was flushed with hydrogen and the sample raised to coating temperature as indicated by an optical pyrometer (corrected for $\rho = 0.4$ at $\lambda = 0.65\mu$). The hydrogen was then sent through the silicon tetrachloride (maintained at the desired temperature) and into the coating chamber. This caused the specimen temperature to drop, requiring readjustment to the desired value. At the end of the coating period, the hydrogen flow was caused to by-pass the silicon tetrachloride and the sample was cooled after flushing the coating chamber with hydrogen.

The life of a coated filament in air was used as a standard in evaluating variables in the coating procedures which are, in many cases, interdependent. The effect of the various factors can be sufficiently isolated, however, to indicate the conditions which tend to give a coating having optimum protective properties.

The compositions of the various layers produced in these coatings were determined by comparison of their metallographic and x-ray analyses with similar analyses of a series of molybdenum-silicon alloys.

RESULTS

In siliconizing molybdenum, two types of coatings are generally obtained, depending primarily upon the coating temperature and to a lesser extent on the gas-flow rate and the concentration of silicon tetrachloride. Below 1420°C, the melting point of silicon, the coating may be either two or three phase, depending on whether or not an outer layer of silicon is obtained. In the three-phase coating, layers of Si, $MoSi_2$, and MoSi are present, while the two-phase coating consists of an outer layer of $MoSi_2$ and an intermediate layer of MoSi. Above the melting point of silicon, only the two-phase coating is normally obtained. However, if deposition is carried out at high gas-flow rates or with high concentrations of $SiCl_4$ in the plating atmosphere, a layer of molten silicon can be obtained. By using low flow rates or low $SiCl_4$ concentrations, the formation of free-silicon coatings below 1400°C can be avoided. A coating of free silicon can be converted into molybdenum silicide by holding the coated sample at a temperature just below the melting point of silicon.

The relative rates of formation of these various layers on a 2-mm-diameter molybdenum wire at 1800°C are shown in Fig. 2.

The total rates of formation of molybdenum silicide coatings at various coating temperatures are shown in Fig. 3. The hydrogen flow rate in this set of experiments was 800 cm^3/min, while that used in obtaining the data in Fig. 2 was 500 cm^3/min.

Examination of Fig. 2 and 3 shows that the deposition rate decreases with time, with the rate of formation of the inner (MoSi) layer diminishing more rapidly than that of the outer ($MoSi_2$) layer. This is

the result of the fact that deposition occurs primarily by displacement, particularly at the higher temperatures.

A photomicrograph of a coating produced at 1800°C is shown in Fig. 4.

Deposition temperatures were not critical, almost identical performance being obtained with wires given coatings of equal thickness at temperatures from 1400°–1700°C.

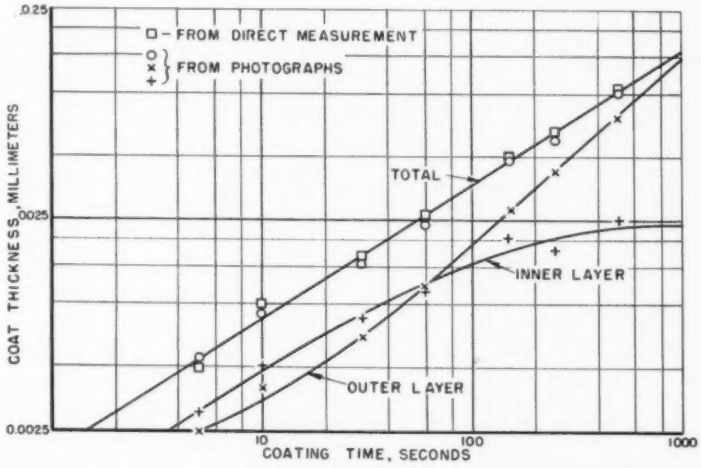

FIG. 2. Effect of coating time on coat thickness for molybdenum wire siliconized at 1800°C.

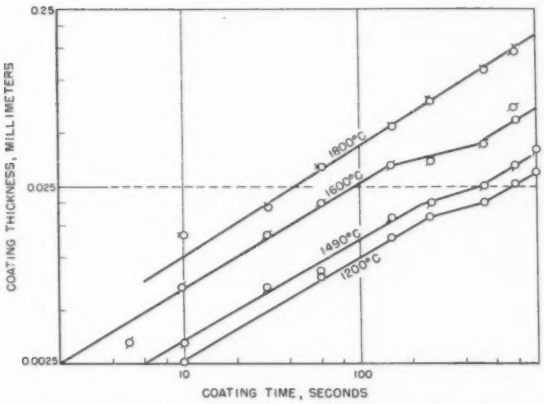

FIG. 3. Effect of coating time on total coating thickness at 1200°, 1490°, 1600°, and 1800° C. Hydrogen flow—800 cm³/min $SiCl_4$ at room temperature.

The concentration of $SiCl_4$ in the coating atmosphere was likewise found to be not critical.

Close control of the rate of gas flow over the sample while coating was not required. A tenfold variation in flow rate had little effect on coating uniformity or test life with the 2-mm-diameter wires. In coating larger objects, however, the flow rates become more critical.

Various methods of cleaning the surface prior to coating had little effect on the test life. Conversely, intentional contamination of the wire before coating, by electrodepositing a thin layer of copper on it, did not noticeably reduce the test life.

The effect of total coat thickness upon the filament life in air is shown for two test temperatures in Fig. 5. These plots can be expressed by the function

$$L = Kt^n$$

where L = life in hours, t = coat thickness in milli-

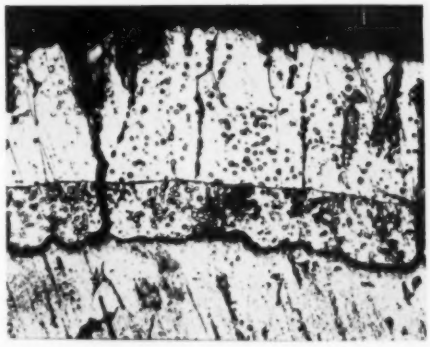

FIG. 4. Silicide layer produced on 2-mm-diameter molybdenum wire at 1800°C. Coating time—250 seconds, H_2 flow rate—500 cm³/min, $SiCl_4$ at room temperature. Etchant 1:1:1 HNO_3-HF-H_2O. 500×.

meters[2]; K = 12,460 at 1200° C and 2,565 at 1700°C, and n = 1.65 at 1200°C and 1.51 at 1700°C. Data for preparing similar plots for coatings on larger or smaller bodies, or for coatings made at temperatures other than 1800°C, are not available.

Judging from Fig. 5, in order to obtain adequate protection at any given temperature, one needs only to apply a sufficiently thick silicide coating. However, this is not the case. Coatings more than 0.075- or 0.100-mm thick have a pronounced tendency to

[2] Obtained from photomicrographs of cross sections of a duplicate set of coated wires.

crack (Fig. 6). This, and other factors, will probably limit the practical coat thickness to less than 0.250 mm. This limit applies to coatings produced on a molybdenum base by the process described here. Other processes capable of producing thicker coatings will be described later.

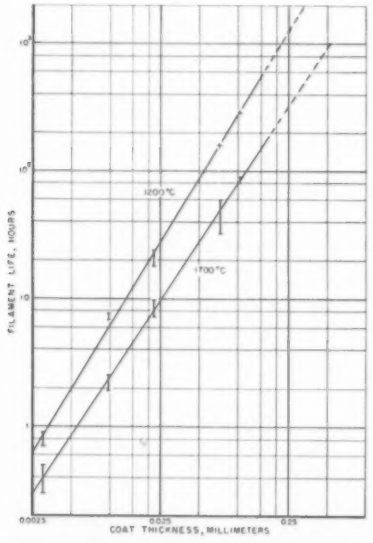

FIG. 5. Effect of coat thickness upon test life in air at 1200° and 1700°C.

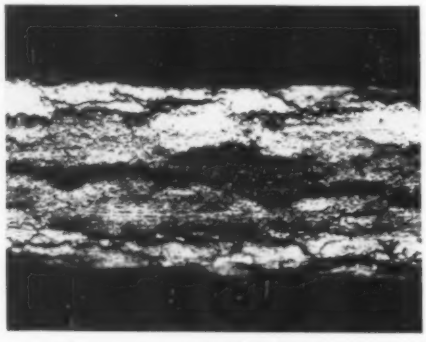

FIG. 6. Photomacrograph showing surface of molybdenum wire siliconized for two hours at 1800°C in a flow of 1500 cm³ per minute of hydrogen saturated with $SiCl_4$ at room temperature. 12×.

For comparison with the data plotted in Fig. 5, the life of an uncoated 2-mm-diameter molybdenum wire in air at 1000°C is about 0.1 hour.

The composition of the test atmosphere had some effect on test life in that slightly longer lives were obtained in atmospheres saturated with water vapor than in dry atmospheres. The difference was not marked, however.

Localized contamination of the coated filament prior to, or during, the oxidation test had a pronounced effect upon filament life. Metallic contaminants were harmful in the order Fe > Cu, Chromel A, Ni > Cr, Mo. Small spots of iron or the other metals, except Cr and Mo, reduced the test lives at 1700°C to a few tenths of an hour, or at best one or two hours. The latter two had little effect on the test life. Nonmetallic contaminants capable of reacting with (fluxing) the SiO_2 film (e.g., CaO) reduced the test life to less than an hour at 1700°C.

Very few oxidation tests have been made to date of siliconized molybdenum specimens under load. Available data on some early tests of 0.025-mm-thick coatings on 2-mm-diameter wires show lives of 500 to 1000 hours at 975°C under 5000-psi load. The coatings have been greatly improved since these tests were made.

While most of the testing has been done by heating the specimens internally, comparable resistance to oxidation is shown by samples heated externally in furnaces and by hot gas flames.

The molybdenum disilicide coating is highly resistant to corrosion by most acids and alkalies. It is slowly attacked by dilute hydrochloric acid and concentrated hydrofluoric acid, however, and is rapidly attacked by a hydrofluoric-nitric acid mixture.

The approximate Knoop hardness values for the various coating layers are (100-g load): Si—940; $MoSi_2$—1160; MoSi—890. While the disilicide is harder than silicon, it is not nearly so brittle. The silicide coatings are semiductile at room temperatures (the coated wire can be bent slightly without cracking the coating), and, at a red heat, the treated wire can be wound into tight coils without damaging the coating. The thermal-shock resistance of the coatings is very good; the coated filaments can be heated from room temperature to 1700°C in a second or less without failure. Any cracks which do appear are self-healing, by reason of a crack-plugging film of SiO_2 which forms on the surface of the silicide.

Discussion

Although this report is primarily concerned with the preparation of molybdenum silicide coatings by vapor-phase deposition, a number of other coating methods have been tried. These include dipping in molten silicon; flame spraying the mixed, or alloy, powders; sintering an overlay of molybdenum silicide; cladding by fusion welding using a molybdenum silicide rod; and electrolysis of fused silicate baths at high temperatures. A few of these processes are promising, especially for applying thicker coatings than can be obtained in a continuous form by the vapor-phase processes.

Conclusion

The siliconizing of molybdenum is a very effective

way of imparting the corrosion resistance of a silica glass to this highly refractory metal. This process offers promise for treating parts subject to ordinary chemical attack and to high-temperature oxidation. These include furnace heater elements, combustion chambers, turbine blades, nozzles, heat exchangers, etc.

These coatings are being continuously improved by further research. The results to date show that lives of over 1000 hours at 1700°C in air are a certainty for molybdenum filaments having silicide coatings less than 0.125-mm thick, and lives of 2000 hours or more are highly probable.

Acknowledgment

The authors wish to extend their appreciation to the Fansteel Metallurgical Corporation for permitting the publication of this report. They also wish to acknowledge the interest and assistance of Dr. B. W. Gonser of Battelle Memorial Institute in the investigation.

Any discussion of this paper will appear in a Discussion Section, to be published in the December 1951 issue of the Journal.

References

1. O. Honigschmid, *Monatsh.*, **28,** 1017, (1908).
2. E. Wedekind and J. Pintsch, German Pat. 294,267, September 12, 1913.
3. J. N. Pring and W. Fielding, *J. Chem. Soc.*, **95,** 1497, (1909).
4. N. V. Philips Gloeilampenfabrieken, British Pat. 200,879, March 24, 1922.
5. N. Parravano and C. Mazzetti, *Rec. trav. chim.*, **42,** 821 (1923).
6. R. Hölbling, *Z. angew. Chem.*, **40,** 655 (1927).
7. G. K. Teal, J. R. Fisher, and A. W. Treptow, *J. Applied Phys.*, **17,** 879 (1946).
8. K. H. Storks and G. K. Teal, U. S. Pat. 2,441,603, May 18, 1948.

Distribution of Current in Porous Electrodes[1]

J. J. Coleman

Burgess Battery Company, Freeport, Illinois

ABSTRACT

An experimental test is made of the applicability of Kirchoff's law to porous electrodes. The theory is applied to a dry cell made with three bodies of mix separated from each other by paper walls wet with electrolyte. The three bodies are thus isolated electronically but connected ionically. All three are connected to the external load. Thus, the electronic current flowing into each body of mix is equal to the polarizing current in each body and hence is a measure of the rate of reduction of manganese dioxide in each body. It is shown that established theory explains the distribution of current, using two parameters determined directly from the current distribution data.

Introduction

This is a continuation of work reported in a previous paper (1) in which the behavior of a dry cell in terms of changes in concentration in the neighborhood of a representative manganese dioxide particle was described[2]. These concentrations are altered first by the current of electrons flowing to the particle and the resulting reduction of the particle and second by diffusion. The main objective of the paper was to explain quantitatively the marked dependence of ampere-hour capacity on rate of discharge as the result of the increased effectiveness of diffusion when the discharge rate is lowered.

As a first step in such an inquiry, one must determine how the rate of reduction of the particle depends on its position. Electrons flow to the particle through the web of black. Some of these electrons are absorbed by the particle and an ionic current is established of equal magnitude. Chemically, we think of the reduction of manganese dioxide to a lower oxide. Electrically, we picture the conversion of an electronic current into ionic current, by what has been called "the polarizing current" (3). The problem can be discussed in either electrical terms or chemical terms. In the paper on dry cell dynamics, the distribution of polarizing current was determined by applying Kirchoff's law to the flow of ionic, electronic, and polarizing current within the porous cathode; and hence, electrical terms were appropriate.

Cahoon and Heise (2) took the *p*H of the electrolyte as an index to the extent of reduction at any point within the mix—although they noted that diffusion of acidic, anodically formed $ZnCl_2$ complicates the situation at the periphery of the mix. They made *p*H measurements on portions of mix taken from partially discharged cells and also analyzed these samples chemically. They confined their attention to a particular flashlight cell discharging continuously on a 4-ohm load.

They concluded that at the beginning of the discharge the rate of reduction is most intense near the carbon rod, and as the discharge proceeds the rate of reaction increases in the middle and outer layers of the bobbin.

Daniel-Bek (3) described the distribution of current in the bobbin the same way as given in the earlier work (1), with one exception. He considered an electronic current in the web of black (dry cells), web of lead (lead storage batteries), etc., and an ionic current in the web of electrolyte. He grouped all of the solids together—the material added to transport the electrons and the oxidizing agent—and called the sum of the two the "active mass." He associated the conversion of electronic current to ionic with a flow of current through the surface of this mass, "the polarizing current." On the other hand, in (1) it was assumed that the polarizing current flowed through the manganese dioxide particles which have a (representative) resistance r. The two analyses become identical when $r \to 0$.

Both analyses lead to the conclusion that when the specific resistances of the web of black and of the web of electrolyte are equal or nearly equal, the polarizing current (at the start of a discharge) is high near the carbon rod, declines to a minimum, and then rises again to a high value near the edge of the core.

Daniel-Bek made the important observation that the mathematical analysis developed is applicable to all kinds of porous electrodes.

Both of these papers contained data obtained by the use of exploring electrodes. This kind of data sometimes proves unconvincing (2) because of the necessary complexity of interpretation. In contrast,

[1] Manuscript received March 20, 1950. This paper prepared for delivery before the Buffalo Meeting, October 11 to 13, 1950.

[2] Possible changes of concentration within the particle itself were also considered.

analyses of samples of mix taken from various portions of the core lead quickly to plausible conclusions. However, in making such conclusions one must keep in mind the fact that we are dealing with a dynamical situation. The processes going on within a cell are not immobilized by opening a switch since diffusion continues. Current may even continue to flow within the mix, the regions of least reduction charging the regions of greater reduction. An ammeter, however, measures a rate and catches an instantaneous picture.

The purpose of this paper is twofold: (*a*) to describe a special type of experimental dry cell in which the distribution of polarizing current can be followed easily and simply by electrical measure-

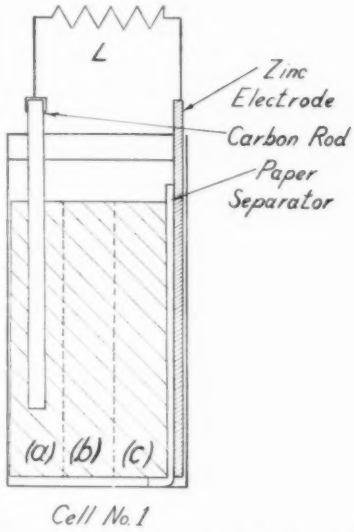

FIG. 1. Cross section of a rectangularly shaped dry cell

ments; (*b*) to show that the resulting data agree with the theoretical principles given before (1).

EXPERIMENTAL

Consider first a cell (Fig. 1, No. 1) employing a rectangular block of mix divided into three equal bodies (*a*), (*b*), and (*c*). We can describe the distribution of polarizing current approximately by stating the total polarizing current absorbed by each division. Let I_a, I_b, and I_c be the polarizing currents absorbed by (*a*), (*b*) and (*c*), respectively. If I is the total current delivered by the cell, then

$$I = I_a + I_b + I_c \qquad (I)$$

This is simply a statement of the fact that all of the electronic current entering the cathode must be converted to ionic current somewhere within the cathode.

Now consider cell No. 2 (Fig. 2) where three bodies of mix are isolated from each other electronically by paper barriers. These barriers are wet with electrolyte and can pass ions but not electrons.

In cell 1 electrons are carried to (*b*) and to (*c*) by the web of black. In cell 2 electrons are carried to (*b*) and to (*c*) by resistors r_1 and r_2. To this extent there is an analogy between r_1 and r_2 in cell 2 and the web of black in cell 1. For example, if r_1 and r_2 are very large compared to the resistance of the electrolyte, most of the polarizing current is concentrated in (*a*). Likewise, if the resistance of the web of black is very large compared to the resistance of the electrolyte in cell 1, most of the polarizing current is concentrated in region (*a*).

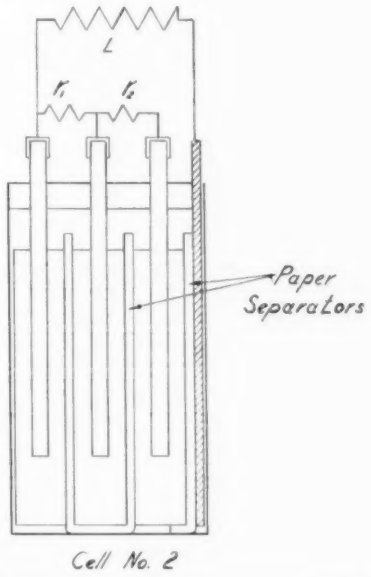

FIG. 2. Cross section of an experimental cell containing three bodies of mix electronically isolated from each other.

Conditions are relatively simple at the beginning of the discharge period. Here all the manganese dioxide particles develop the same emf and the specific resistance to ionic flow is everywhere the same in the cathode; no blocking precipitates have been formed. This simple state of affairs is very well suited for checking some of the theory of porous electrodes in its present crude state and this paper is confined to this region, i.e., to a consideration of fresh undischarged cells.

Three slabs of mix 5.08 cm by 4.45 cm by 0.953 cm were used in the experimental cell (Fig. 2). The mix was composed of 90 parts African ore, 10 parts acetylene black, 15 parts of ammonium chloride, and 48 parts of a solution which contained 22 per cent $ZnCl_2$ and 28 per cent NH_4Cl. Various combinations of r_1, r_2, and L (see Fig. 2) were tried. Potentials across r_1 and r_2 were measured by millivoltmeters

having a resistance of one million ohms per volt. The potential across L was also measured. From these measurements it was easy to calculate I, I_a, I_b, and I_c. Results are shown in Table I.

In the first four sets of data $r_1 = r_2$ but in the last two this condition does not hold. When $r_1 = r_2$ there is, of course, no analogy with a simple cell such as shown in Fig. 1. In the last set of data, I_b is negative. This means that electrons flowed out of slab (b) instead of into it. The significance of this set of data is considered later.

TABLE I. *Measured distribution of polarizing current*

r_1	r_2	I	I_a		I_b		I_c	
ohms	ohms	(ma)	(ma)	%	(ma)	%	(ma)	%
0.25	0.25	16.8	0.8	5*	2.8	17*	13.2	78*
		32.4	7.6	23	4.8	15	20	62
		63.2	19.2	30	10.8	17	33.2	53
		121.6	40.4	33	21.2	17	60	49
0.50	0.50	16.7	5.7	34	5.6	33	5.4	33
		32.5	13.1	40	9.4	29	10	31
		62.8	27.4	44	15.4	24.5	20	32
		120	55	46	27	22.5	38	32
1.0	1.0	16.8	9.8	58	3	18	4	24
		32.6	19.6	60	5	15	8	25
		59.5	35.5	60	10	17	14	23
		115.2	69.2	60	20	17	26	23
2.0	2.0	16.7	11.7	70	3	18	2	12
		32.3	23.3	72	4.5	14	4.5	14
		61.6	45.6	74	7	11	9	15
		118.0	90	76	13	11	15	13
0.5	1.0	16.6	7.6	46	5	30	4	24
		31.8	14.8	46	9.5	30	7.5	24
		62.3	30.3	49	17	27	15	24
		118.3	57.3	48	33	28	28	24
4	0.25	16.5	13.5	82	−7	−42	10	60
		32.2	24.2	75	−6.8	−21	14.8	46
		62.3	51.3	82	−13	−21	22	39
		122.3	110.8	90	−12.5	−10	24	20

* Not considered in the averages shown in Table II.

Theory

Consider briefly what information can be derived from the analogy between cell 1 and cell 2. Note first that the per cent values for I_a, I_b, and I_c apparently depend only on r_1 and r_2, and are independent of the load on the cell. (See Table I. The last set of data does not follow this rule.) For example, when $r_1 = r_2 = 1.0$ about 60 per cent of the polarizing current is absorbed by slab (a) whether the load is 16.8 ma or 115.2 ma. A sevenfold increase in the load does not change the fraction of the current absorbed by a, b, and c. In Table II there are listed the average per cent values for I_a, I_b, and I_c.

I_b tends to be lower than either I_a or I_c and it can be concluded that the initial flow of polarizing current in cell 1 shows a minimum somewhere in the mid-region between the carbon rod and zinc electrode. Further, if the percentage values of I_a, I_b, and I_c found for cell 2 are assigned to the mid-points of regions (a), (b), and (c) in cell 1, as in Fig. 3, then the points are connected by simple curves.

TABLE II. *Distribution of polarizer current (experimental)*

r_1	r_2	I_a	I_b	I_c
ohms	ohms	%	%	%
0.25	0.25	29	16	55
0.50	0.50	41	27	32
1.0	1.0	60	17	23
2.0	2.0	73	13	14
0.5	1.0	47	29	24

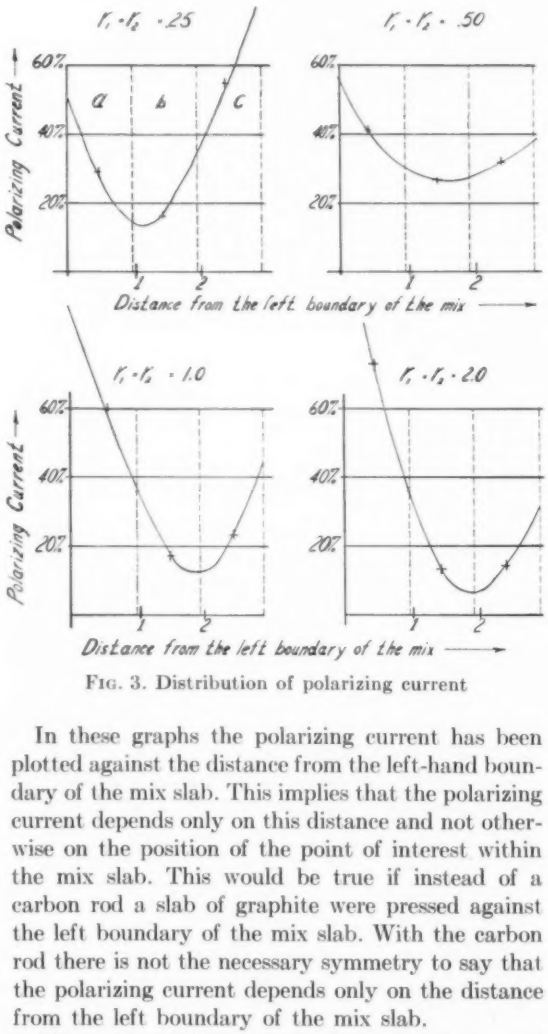

Fig. 3. Distribution of polarizing current

In these graphs the polarizing current has been plotted against the distance from the left-hand boundary of the mix slab. This implies that the polarizing current depends only on this distance and not otherwise on the position of the point of interest within the mix slab. This would be true if instead of a carbon rod a slab of graphite were pressed against the left boundary of the mix slab. With the carbon rod there is not the necessary symmetry to say that the polarizing current depends only on the distance from the left boundary of the mix slab.

The carbon rod reaches nearly to the bottom of

the mix slab. Hence, there is enough symmetry in the vertical direction to say that the polarizing current is virtually independent of the vertical position. It is the direction vertical to the paper in Fig. 2 which lacks the proper symmetry for a simple interpretation of the curves in Fig. 3. This is direction y in Fig. 4. However, each point on a curve in Fig. 3 represents the polarizing current x cm from the left-hand boundary of the mix averaged over all values of y.

Thus, this gives an interpretation of the curves in Fig. 3 in terms of cell 1 and in terms of a cell with a simpler geometry, i.e., a cell with a graphite slab replacing the carbon rod.

The same method of anlaysis is employed in a quantitative study of cell 2, the cell to which the experimental data apply directly, to develop a theory for this cell as was done previously (1) to determine the distribution of current in a dry cell with a cylindrical bobbin. The dependence of I_a, I_b, and I_c upon r_1 and r_2 can be established and the theoretical values of these currents are found to agree well with the measured values. This gives support to the belief that the method of analysis used is correct for all sorts of porous electrodes.

The necessary fundamental equations are derived by the application of Kirchoff's law, that the emf's and IR drops in any closed path in an electrical circuit must balance. One such closed path can be constructed as follows: Start with a dioxide particle very near to the carbon rod in slab (a); proceed up the carbon rod through r_1 and down the carbon rod in (b) to a very near dioxide particle; proceed through the particle to the electrolyte solution; proceed through the solution to the initial starting point.

This path is so constructed that the portion lying in the web of black is negligible. Consider next the IR drop associated with the path through the electrolyte solution. Let i be the ionic current density at any point in slab (a). From symmetry considerations it is evident that i is directed perpendicularly to the zinc electrode except for deviations required by the carbon rod. The errors introduced by this deviation are discussed below. There is a dependence of i upon x and y but not upon the vertical position of the point of interest. Consider first the dependence of i upon x. At the left-hand boundary where $x = 0$, $i = 0$. As x increases, i increases; it is increased at each point within the mix slab by the polarizing current and i may be taken as proportional to x. One could make a more exact analysis similar to that employed previously for a cylindrical bobbin (1); but such an analysis would be much more complex because of more complicated geometry. A long detailed mathematical analysis is neither required nor justified with dry cell theory in its present crude state.

There is also a dependence of i upon y. If the web of black has a very high resistance then i will be large near the center of the slab and smaller in more remote regions. It turns out that one can avoid a detailed consideration of the dependence of i on y by the following artifice. Attention is confined to the portion of the slabs in the center, contained between the two dotted lines in Fig. 4. Let the area of the cross section, parallel to the zinc electrode for this portion, be a and the total cross-sectional area of the slab be A. One can then put

$$i = \alpha \frac{a}{A} \frac{x}{s} I_a. \qquad \text{(II)}$$

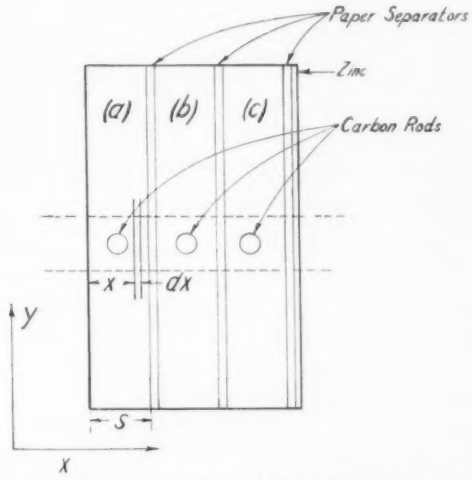

FIG. 4. Cross section of experimental cell vertical to that shown in Fig. 2.

If i is uniformly distributed with respect to y, i.e., if i is independent of y then $\alpha = 1$. Whatever the value of α it should be the same for all three slabs. Having established approximation (II) it is easy to calculate the required IR drop. The drop across the lamina of thickness dx shown in Fig. 4 is $widx$ where w is the specific resistance of the web of electrolyte and the total drop from the center of the electrode in (a) to the center of the electrode in (b) can be obtained by integration. This requires the lamina to take positions where i is bent by the carbon rods. However, the effect here is to decrease the current density in the center of the lamina and to increase it at the edges. This effect is negligible.

Turn now to the IR drop produced within the dioxide particle by the polarizing current. Each particle has an individual resistance but it is sufficiently accurate to treat them all as having a single resistance, r. In the lamina shown in Fig. 4 there are $vadx$ particles, where v is the number of particles

per unit volume. The total polarizing current flowing through these particles is $di = \alpha(a/As)I_a dx$. All of the particles within the lamina are, as it were, connected in parallel; hence the IR drop is

$$\frac{r}{vadx}\,\frac{\alpha a I_a\,dx}{As} = \frac{r\alpha}{vsA}\,I_a = \alpha\beta I_a \qquad \text{(III)}$$

where

$$\beta = \frac{r}{vsA} \qquad \text{(IV)}$$

simply the resistance of all of the particles within the slab taken as connected in parallel.

TABLE III. *Distribution of polarizing current (theoretical)*

r_1	r_2	I_a	I_b	I_c
ohms	ohms	%	%	%
0.25	0.25	33	25	42
0.50	0.50	43	23	34
1.0	1.0	56	19	25
2.0	2.0	70	15	15

The application of Kirchoff's law is quite straightforward from this point on and one finds

$$\left(\alpha\beta + \frac{7}{8}\,\frac{\alpha s w}{A}\right) I_a + \left(\frac{1}{8}\,\frac{\alpha w s}{A} - \alpha\beta - r_1\right) I_b - r_1 I_c = E_a - E_b \qquad \text{(V)}$$

$$\frac{\alpha w s}{A}\,I_a + \left(\alpha\beta + \frac{7}{8}\,\frac{\alpha w s}{A}\right) I_b + \left(\frac{1}{8}\,\frac{\alpha w s}{A} - r_2 - \alpha\beta\right) I_c = E_b - E_c \qquad \text{(VI)}$$

in which E_a, E_b, and E_c are the electromotive forces developed by the respective slabs. At the start of the discharge $E_a = E_b = E_c$, and one gets from (I), (V), and (VI)

$$I_a/I = \frac{(m+n)r_1 + mr_2 + r_1 r_2 + m^2}{D} \qquad \text{(VII)}$$

$$I_b/I = \frac{-pr_1 + nr_2 + nm}{D} \qquad \text{(VIII)}$$

$$I_c/I = \frac{pr_1 + mp + n^2}{D} \qquad \text{(IX)}$$

in which

$$D = r_1 r_2 + (m+n)(r_1 + r_2) + n(2m+n)$$

$$m = \alpha(\beta - ws/8A) \qquad \text{(X)}$$

$$n = \alpha(7ws/8A + \beta) \qquad \text{(XI)}$$

$$p = \frac{\alpha w s}{A}. \qquad \text{(XII)}$$

Equations (VII), (VIII), and (IX) are rather complex but it is possible to draw one important conclusion, namely, that the fractional values of the polarizing currents I_a, I_b, and I_c are independent of the total load I. This is a particular case of a general theorem and conforms to the experimental observation made above.

To test the equations further values of $\alpha\beta$ and αw are needed. These can readily be found from the equations

$$(I_a - I_b)\alpha\beta + (\tfrac{7}{8}I_a + \tfrac{1}{8}I_b)\,\frac{\alpha w s}{A} = r_1(I_b + I_c) \qquad \text{(XIII)}$$

$$(I_b - I_c)\alpha\beta + (I_a + \tfrac{7}{8}I_b + \tfrac{1}{8}I_c)\,\frac{\alpha w s}{A} = r_2 I_c \qquad \text{(XIV)}$$

which follow from (V) and (VI) when $E_a = E_b = E_c$.

Using these equations and all of the data in Table I except the last set ($r_1 = 4$, $r_2 = 0.25$) one finds

$$\alpha\beta = 0.68 \text{ ohm} \qquad \text{(XV)}$$

$$\alpha w = 8.30 \text{ ohms cm} \qquad \text{(XVI)}$$

The specific conductivity of the electrolyte used is about 0.345 ohm^{-1} cm^{-1}. In one cm^3 of mix there are 0.487 cm^3 of electrolyte. Hence, the specific conductivity of the web of electrolyte is approximately $0.487 \times 0.345 = 0.168$ or $w = 5.95$ ohms cm. This gives $\alpha = 1.39$, $\beta = 0.498$ ohms, $r/v = \beta sA = 10.6$ ohms cm^3.

Since α is greater than 1, this indicates that the region near the carbon rod is one in which the polarizing current is high. The geometry of the cell leads directly to the same conclusion.

Table III gives calculated values for I_a, I_b, and I_c based on the values of α, β, and w given above. The agreement with the experimental values given in Table II is fairly good.

The negative sign in equation (VIII) leads to the curious conclusion that if r_1 and r_2 are chosen correctly, it should be possible to reverse the current in slab (b); that is a "charging" current should flow into slab (b) when a load is put on the cell. For example when $r_1 = 4$ and $r_2 = 0.25$, then the calculated current distribution is

$$I_a = 80\%$$
$$I_b = -5\%$$
$$I_c = 25\%$$

Experimental values are given in Table I. There is certainly no quantitative agreement with theory, but the predicted charging current is observed.

Any discussion of this paper will appear in a Discussion Section, to be published in the December 1951 issue of the JOURNAL.

REFERENCES

1. J. J. COLEMAN, *Trans. Electrochem. Soc.*, **90**, 545 (1946).
2. N. C. CAHOON AND G. W. HEISE, *J. (and Trans.) Electrochem. Soc.*, **94**, 214 (1948).
3. V. S. DANIEL-BEK, *J. Phys. Chem. U.S.S.R.*, **22**, 697 (1948); *C. A.*, **42**, 7642a (1948).

Rate of Dissolution of Silver in Aqueous Ceric Sulfate Solutions[1]

HUGH W. SALZBERG, HELEN KNOETGEN, AND ANN M. MOLLESS

Hunter College, New York, New York

ABSTRACT

The dissolution of silver and copper in ceric sulfate is diffusion controlled, in contrast to the dissolution in ferric sulfate solutions, which is desorption controlled. This is thought to be due to a greater heat of reaction which supplies sufficient energy for immediate desorption of ions produced in the course of reaction.

By analogy with silver, reactions between oxidants and metals with small differences in standard oxidation potential should be desorption controlled. Reactions between oxidants and metals with large potential differences should be diffusion controlled.

INTRODUCTION

The dissolution of a metal in a solution containing an oxidant is the result of three consecutive processes. These are the transport of oxidant to the surface, chemical reaction at the surface, and removal of the reaction products from the surface. The slowest of these processes will determine the rate.

When the transport of material is the rate-determining step, the process is termed "diffusion control" (1). The generally accepted criteria of diffusion control are as follows (2, 3):

1. Different solids dissolve at nearly the same rate in the same reagent under the same conditions.
2. The speed of stirring has a large effect, the exact nature of which depends on the type of stirring used. The graph of rate versus stirring speed does not reach a maximum, but increases continuously.
3. The dissolution rates with a series of reagents are proportional to a fractional power of the diffusion coefficient (about 0.75).
4. The dissolution rate is inversely proportional to the viscosity, other factors remaining constant.
5. The temperature coefficients are lower than for homogeneous reactions, usually between 1.1 and 1.5 per ten-degree rise in temperature.
6. The dissolution rate increases with increasing concentration of reagent, the curve being linear.
7. The previous treatment of the surface has only a very minor effect, if any.
8. All faces of crystals dissolve at the same rate.
9. Diffusion-controlled rates are generally higher than nondiffusion-controlled rates.

The over-all rate equation for a diffusion-controlled process may be expressed as $dx/dt = KA(a-x)V$, where A is the surface area, in square centimeters, of the metal being dissolved, a is the original concentration of oxidant in gram-ions/liter, x is either the concentration of product being formed or the concentration of reagent that has disappeared during the course of the reaction, and V is the volume, expressed in liters. K is the specific rate constant expressed in $cm^{-2} min^{-1}$ and depends upon the temperature, stirring speed, viscosity, and the particular materials involved.

Nondiffusion-controlled reactions have previously been referred to as "chemically-controlled" reactions. However, strictly speaking, this should refer only to those cases in which the rate-determining step is the actual chemical reaction (electron transfer). There is as yet no clear-cut case of true chemical control.

Cases where the slowest or rate-determining step is the removal of material from physical contact with the surface should be considered to be under "desorption control." One clear-cut case of this has already been reported (4) and others are being investigated. From consideration of the criteria for diffusion control and the actual results in the above-mentioned case of desorption control, the criteria for the latter are as follows:

1. Different solids dissolve at different speeds in the same solution, under the same conditions.
2. The speed of stirring has a slight effect, but not as pronounced as in diffusion control.
3. The dissolution rates should not be dependent on the diffusion coefficients of the reagents.
4. The dissolution rate is independent of viscosity, until the solution becomes so viscous that the rate of transport is slower than the rate of desorption.
5. The temperature coefficients are much higher than in diffusion control, the value being anywhere between 2 and 4 per ten-degree rise in temperature.
6. The dissolution rate increases with reagent con-

[1] Manuscript received June 13, 1950. This paper prepared for delivery before the Buffalo Meeting, October 11 to 13, 1950.

centration in a nonlinear fashion, slowly and reaching a maximum.

7. The previous condition of the surface has a very marked effect. For example, a polished surface gives a higher rate than an unpolished one.

8. Different crystals dissolve at different rates (5).

9. Desorption-controlled rates should in general be slower than diffusion-controlled rates.

There has as yet been no development of a general rate equation for desorption control.

In the previous work on dissolution of metals in ferric sulfate solutions (6, 4) it was found that the

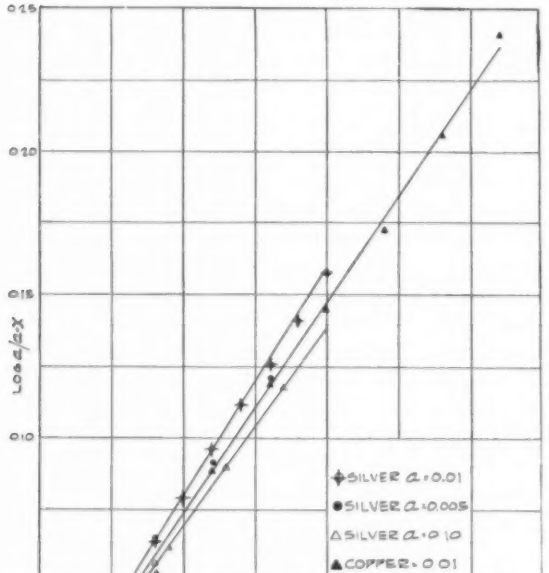

FIG. 1. Log $a/a-x$ versus time

ferric ion oxidized a series of metals at diffusion-controlled rates. Silver, however, was an exception, subject to desorption control. The immediate explanation was the fact that there were large differences in potential between the oxidizing ferric-ferrous system and the metal-metal ion system in diffusion-controlled cases. For example, in the dissolution of copper by ferric ion, the standard oxidation potential difference is 0.404 volts. In the case of silver, the standard potential difference is only 0.050 volts and the reaction is desorption controlled.

Consequently, it was felt that a study of the kinetics of the ceric-cerous oxidation of silver, where the potential difference is 0.75 volts, would tend to either corroborate or disprove this apparent dependence of dissolution rate upon oxidation potential. The present study was undertaken, therefore, to determine the type of control and to attempt to correlate reaction rate and oxidation potential.

The stoichiometric equations for the reactions are

$$Ag + Ce^{++++} \rightarrow Ag^{+} + Ce^{+++}$$

and

$$Cu + 2Ce^{++++} \rightarrow Cu^{++} + 2Ce^{+++}.$$

EXPERIMENTAL

The experimental method was that of rotating a metallic cylinder at constant speed and temperature in solutions of known concentration, as in the previous work on silver dissolution in ferric sulfate (4). Rotational speed was controlled by a Variac and

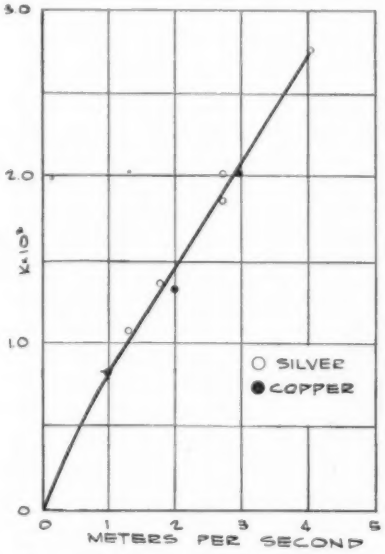

FIG. 2. Rate versus peripheral speed

measured with a flashing neon bulb. Rotational rates used were only those in resonance with sixty-cycle current. Temperature variations during runs were so slight that it was not found necessary to use a thermostat.

The reagents were chemically pure, and 250 cm³ of solution were used for each test. This volume was a compromise figure so that sufficient metal would dissolve to change the ceric sulfate concentration while the cylinder did not suffer excessive loss of metal and consequent change in peripheral speed. The solutions were made by diluting a stock solution 0.215N in ceric ion and 5N in sulfuric acid. Sufficient additional acid was put in each solution to prevent hydrolysis on dilution.

Polishing before runs had no discernible effect and, therefore, the cylinder was not polished before runs, merely being cleaned in acid.

Results

From Fig. 1 it is apparent that both silver and copper dissolve at rates first order with respect to concentration. For concentrations of ceric sulfate between 0.01*N* and 0.005*N*, calculations show that the constant is the same. Also it is seen that the difference between the *K* of silver at 0.1*N* and that at 0.01*N* ceric sulfate is due to the increased viscosity. The difference in *K*'s between copper and silver is due to the different peripheral speeds.

On increasing peripheral speeds above a few hundred revolutions per minute, during which the effect of eddy currents on the diffusion layer is quite marked, there is a linear increase in rate as shown in Fig. 2. The curve, as is normal for diffusion control, has no maximum and the values for both silver and copper fall on the same curve. It is apparent, therefore, that both silver and copper dissolve at approximately the same rate in ceric sulfate, another indication of diffusion control.

TABLE I. *Rate versus temperature, silver cylinder*

Temp	Speed	Area	$k' \times 10^3$	$K \times 10^3$
°C	meters/sec	cm²		
20	2.65	8.89	5.96	1.55
25	2.71	9.06	7.98	2.02
25	2.68	9.00	7.29	1.86
30	2.67	8.93	9.03	2.33
35	2.66	8.90	10.0	2.58
35	2.66	8.90	10.2	2.62

TABLE II. *Rate versus viscosity, silver at 25°C, viscosity increased by addition of sulfuric acid*

Acid	Relative viscosity	*a*	$K \times 10^3$	Speed
cm³				meters/sec
6.5	1.11	0.01	1.86	2.68
15	[1.19]	0.10	1.77	2.72
16.5	1.20	0.01	1.68	2.66
31.5	1.57	0.01	1.41	2.66
46.5	2.02	0.01	1.00	2.65

As shown in Table I, the rate increases with temperature at about 40 per cent per ten-degree rise in temperature at 25°C.

The viscosities in Table II are relative to water at 25°C, as measured with an Ostwald viscometer. The value in brackets, that for 15 cm³ of acid, was obtained from a plot of viscosity versus added acid.

From these results it is evident that the rate varies inversely with viscosity as is to be expected from diffusion control. These data indicate that the low value of *K* for 0.10*N* ceric sulfate, in Fig. 1, was due to increased viscosity, as mentioned above.

Fig. 3 shows the comparison of the rates of silver oxidation by ceric sulfate with those of silver oxidation by ferric sulfate. The latter results were obtained from the previous work (4). The rates in ceric sulfate solution were not measured directly, the values being calculated from the constant picked off the rate-stirring speed curve at 3.00 meters/sec. These rates are only approximate; however, they do give a comparison at least semiquantitative.

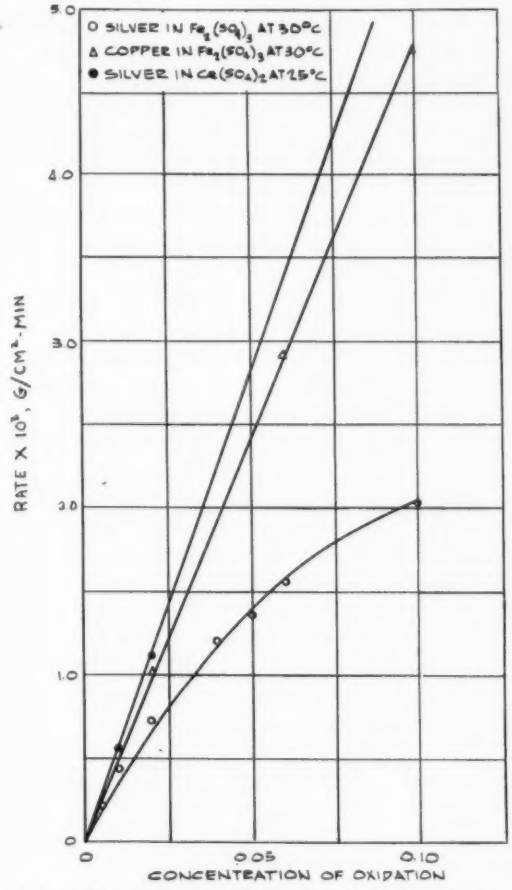

Fig. 3. Rate versus concentration of oxidant, in g-ion/liter.

It may be seen from Fig. 3 that the rates for the ceric ion oxidation are much higher than for the ferric ion oxidation, even though the temperature in the former case is five degrees lower. The difference between the two increases at increased concentrations as the value for the ferric ion oxidation deviates increasingly from diffusion control. For purposes of comparison, the value for diffusion control in ferric sulfate, as determined with copper metal, is included in the graph as the central straight line. The fact that the diffusion-controlled values of ceric sulfate at 25°C are greater than those for ferric sulfate at 30°C indicates either that the activity coefficient for the former is greater or that the ferric

ion forms a complex which is heavier than the ceric ion or any of its complexes.

Discussion

The experimental results show the following:

1. Both silver and copper are oxidized by ceric sulfate at rates first order with respect to concentration of oxidant.
2. Both silver and copper dissolve in ceric sulfate at substantially the same rate at the same temperature, concentration, and stirring speed.
3. For both silver and copper there is a marked stirring effect, the curve of rate versus stirring speed being linear above the first few hundred revolutions per minute.
4. For silver there is a low temperature coefficient, being about 1.4 per ten-degree rise in temperature at about 25°C.
5. The rate of dissolution of silver varies inversely with the viscosity of the solution.
6. The rate of silver dissolution in ceric sulfate is much greater than that in ferric sulfate solution, the latter being known to be desorption controlled.
7. The dissolution of silver in ceric sulfate is not affected by previous treatment of the silver surface, polishing having no discernible effect.

Seven of the nine criteria for diffusion control being satisfied, it is apparent that the dissolution of both silver and copper in ceric sulfate is diffusion controlled. It is to be regretted that we were unable to test the other two criteria, materials and apparatus being unavailable.

The results of this investigation would thus tend to corroborate the idea that a large difference in oxidation potential between the metal and the solution facilitates diffusion control, while a small difference results in desorption control.

The explanation of this effect would seem to be as follows. Since the free energy of a reaction, DF, is equal to the difference between the heat of reaction and the product of temperature and entropy change, $DH—TDS$, and since the entropy increase during the reaction is small (about 3 cal/mole/degree, 2 cal for formation of a mole of silver ions, and about 1 cal as the entropy of diffusion or mixing) the free energy may be taken as being approximately equal to the heat of the reaction—900 cal. The potential difference being a measure of the heat of reaction, therefore, a low oxidation potential implies a small heat of reaction and vice versa.

Now, as a result of the reaction, a reagent particle, having struck a silver atom and oxidized it, has between it and the surface a silver ion which is bound to the rest of the metal surface by adsorption. The heat of reaction is shared between the oxidant and the silver ion, increasing the kinetic energy of the former so that it diffuses away almost immediately and decreasing the energy needed by the latter for desorption. Where the heat of reaction is sufficiently large, the share picked up by the silver ion is sufficient to cause immediate desorption, leaving the surface free to react. This then is what happens in diffusion control. When the heat of reaction is only slight, the metal ion does not leave the surface immediately, but has to be activated by collisions with solvent molecules, a relatively slow process. This is desorption control.

This does not imply a direct connection between thermodynamics and rate of reaction. A close inspection of the situation shows that the heat of reaction only determines the mechanism by which the product leaves the surface, not the rate of its leaving.

It is of interest to digress temporarily and note that the above concept offers an explanation of the work of Centneszwer and Heller (7) who found that increasing the stirring speed in a diffusion-controlled reaction resulted in an increased reaction rate no matter how high the speed was originally. The curve they observed apparently had no maximum. This was in contradiction to the idea that increasing stirring speed increases the transportation rate and eventually results in a transport rate so great that "chemical control" ensues. The explanation seems to be that in the case of diffusion control, the large heat of reaction enables the product to leave the surface as rapidly as the reagent arrives, so the surface is continuously clear and able to react.

In the previous work on silver in ferric sulfate solutions it was found that diffusion control of this reaction was exerted in dilute solutions in the absence of reaction product. In these cases the emf exceeded a value of about 0.10 volt. For this value of the emf the heat of reaction can be calculated to be approximately 40 cal/mole, which should be equal to or greater than the heat of desorption. Unfortunately, the proportion of the reaction energy picked up by the oxidant is not known, so that it is not possible to estimate the heat of absorption from this data. However, it may be taken as an estimate that when the heat of reaction exceeds this value, or rather when the potential difference exceeds 0.10 volt, diffusion control should be exerted. Additional work is being done on systems more nearly approaching this potential difference which it is hoped will be reported shortly.

Acknowledgment

The authors' gratitude is hereby expressed to the Hunter College Chemistry Department, which furnished laboratory space and much equipment and to Professor Cecil V. King for his invaluable advice and

suggestions on what was primarily an outgrowth of his own long-time interest.

Any discussion of this paper will appear in a Discussion Section, to be published in the December 1951 issue of the JOURNAL.

REFERENCES

1. W. NERNST, *Z. physik. Chem.*, **47,** 52 (1904).
2. C. V. KING AND M. M. BRAVERMAN, *J. Am. Chem. Soc.*, **54,** 1744 (1935).
3. C. V. KING, Paper presented at the University Conference on Corrosion, Chicago (June, 1947).
4. C. V. KING AND H. W. SALZBERG, *J. Electrochem. Soc.*, **97,** 200 (1950).
5. A. T. GWATHMEY AND A. F. BENTON, *Trans. Electrochem. Soc.*, **77,** 219 (1940).
6. R. G. VAN NAME AND D. V. HILL, *Am. J. Sci.* (4), **42,** 307 (1916).
7. M. CENTNESZWER AND W. HELLER, *Z. physik. Chem.*, **A161,** 113 (1932).

THE ELECTROCHEMICAL SOCIETY, INC.

The Electrochemical Society is an international organization of individuals and companies concerned with or interested in Electrochemistry and allied subjects.

The Society is dedicated to the advancement of the theory and practice of Electrochemistry and related subjects, as shown in the following divisions:

Battery	Electro-Organic
Corrosion	Electrothermic
Electric Insulation	Industrial Electrolytic
Electrodeposition	Theoretical Electrochemistry
Electronics	

Among the means to this end are the holding of meetings for the reading and discussion of professional and scientific papers on these subjects, the publication of such papers, discussions, and communications as may seem appropriate, and cooperation with chemical, electrical, and other scientific and technical societies.

It is an incorporated society without capital stock. The affairs of the Society are managed by a Board of Directors under a Constitution and By-Laws. Officers are nominated by a nominating committee appointed by the Board of Directors and elected by the members.

Direct all general correspondence and inquiries regarding membership to Society headquarters at 235 West 102nd Street, New York 25, N. Y., c/o Mr. W. J. Holian, Assistant Secretary.

Officers of the Society

President ..... CHARLES L. FAUST
Past President ..... ALFRED L. FERGUSON
Vice-President ..... RALPH M. HUNTER
Vice-President ..... J. C. WARNER
Vice-President ..... ROBERT J. MCKAY
Treasurer ..... E. GIDEON WIDELL
Secretary ..... HENRY B. LINFORD